

Rotating-frame transformations: A new approximation for multiphoton absorption and dissociation in laser fields

K. B. Whaley and J. C. Light

*The James Franck Institute and the Department of Chemistry, University of Chicago,
Chicago, Illinois 60637*

(Received 31 January 1983)

The time-dependent Schrödinger equation for the coherent interaction of a multilevel molecular system with an intense electromagnetic field is transformed with a new rotating-frame transformation into a frequency-dependent representation in which much of the information relevant to multiphoton excitation is contained in a time-independent interaction matrix, the solution of which follows by standard eigenvalue techniques. The flexibility of this transformation and simplicity of the resulting approximation (the general rotating-frame approximation) make it a powerful tool for solving the multiphoton dynamics of many-level systems. Extension to interactions with several laser fields is straightforward. The theory is illustrated by application to the model of Schek, Jortner, and Sage [Chem. Phys. 59, 11 (1981)] for the multiphoton dissociation of a diatomic molecule. The results from the general rotating-frame approximation are in good agreement with the exact results obtained by numerical integration of the full time-dependent Schrödinger equation. The implications for treatment of multiphoton absorption and dissociation of polyatomic molecules are discussed.

I. INTRODUCTION

The quantum dynamics of molecular multiphoton absorption and dissociation of polyatomic molecules by intense infrared radiation have continued to generate a substantial amount of theoretical interest, although the qualitative features of the multiphoton excitation process are largely well understood.¹ One of the main challenges facing a quantitative analysis of these processes is the extreme complexity of the molecular level structure. Since this is one of the prime characteristics enabling multiphoton absorption to lead to eventual dissociation in small polyatomics, it is clear that a complete theoretical understanding requires a unified description of multiphoton excitation in both the sparsely populated lower molecular-energy-level region, and in the densely populated upper region, the so-called "quasicontinuum."

Recent theoretical treatments for polyatomic molecules have distinguished initial coherent nonresonant excitation in the lower, sparsely populated level region from a subsequent incoherent resonant excitation process in the quasicontinuum.¹⁻³ Incoherent excitation is consistent with the observed dependence of dissociation probability on laser fluence rather than on laser intensity,⁴ which justifies the use of population rate equations to describe excitation.^{1,5} Such kinetic formulations may be arrived at by both statistical and quantum treatments and, in combination with Rice-Ramsberger-Kassel-Marcus (RRKM) analysis, have been used to simulate the multiphoton dissociation of SF₆.³ However, although it is clear that the presence of the quasicontinuum is related to the very rapid increase in density of states, the transition from the discrete to the quasicontinuous molecular-energy-level region is not a precise concept and there is no sharp point at

which the onset of incoherent excitation may be said to occur. This transition is usually described by a phenomenological decay width related to the rate of intramolecular vibrational energy redistribution (IVR) at an energy determined by the condition that the dephasing rate (rate of IVR) is greater than the Rabi frequency at that energy. Furthermore, although the dissociation probability depends primarily on laser fluence, there is a significant residual dependence upon laser intensity which has not yet been satisfactorily explained.⁴

The rate equation formalisms have been of great advantage in describing the qualitative features of multiphoton excitation and dissociation, and also raise important questions such as the thermal or nonthermal nature of the vibrational state distribution.^{1,6} But the microscopic features of the coupling of the molecular quasicontinuum to the radiation field can at best be described in an averaged sense by such descriptions. This is true for the quantum-mechanical models of random coupling between molecular continua as well as for the statistical treatments. The resonant nature of the coupling in the quasicontinuum and the overall apparent incoherence of the excitation here are important features, but to go beyond a schematic approach toward excitation here, it is necessary to return to an exact quantum-mechanical treatment of the entire excitation process.

Also, incoherent excitation may be sufficient but not necessary for the fluence dependence of dissociation. Excitation by incoherent processes is not the only mechanism for loss of coherence in level populations. For example, irreversible decay of the final state in an absorptive process can also lead to loss of coherence of the molecular populations at high intensities.⁷ Thus it is worth reconsidering coherent excitation processes, provided some way of accurately representing the high density of states for

polyatomic molecules may be found.

Investigation of generalizations of the rotating-wave approximation (RWA) to many-level systems in the presence of one or more laser frequencies has led to some useful insights concerning methods of approaching the time evolution of such a coherent radiation-matter system. It was recognized by Einwöhner, Wong, and Garrison⁸ in 1976 that elimination of the time dependence in the Hamiltonian considerably simplifies the problem of solving for the molecular eigenfunctions. In an important but largely neglected study they investigated the conditions under which this could be done exactly for all except antiresonant interactions.⁸ In general it is not possible to eliminate the entire time dependence of the Hamiltonian. Most numerical studies based on this approach have been restricted to the few special situations for which a tridiagonal time-independent interaction matrix is obtained,⁹ the specific structure of which sometimes allows analytic solutions. However, when applied to the coherent monochromatic multiphoton excitation and dissociation of a strongly anharmonic system such as a diatomic molecule, such a tridiagonal RWA was found to give a very poor description of the excitation and dissociation dynamics when compared to the exact calculation using the full dipole-interaction matrix, together with numerical integration of the full time-dependent Schrödinger equation.¹⁰

Even though the periodicity of the interaction limits the time interval over which one needs to integrate to the period of the incident radiation (provided this is short relative to the interaction time), and use of the Magnus expansion may reduce the number of integration steps required to achieve convergence, such an exact calculation is clearly not feasible for systems more complicated than a diatomic molecule. It is already a very cumbersome and time-consuming process for a realistic diatomic. Indeed all *ab initio* quantum-mechanical treatments of multiphoton excitation processes which explicitly use the entire molecular-level structure have been restricted so far to studies of multiphoton absorption and dissociation of diatomic molecules. Floquet analysis has provided a straightforward and useful way of studying the long-time behavior of molecular-state populations in absorption,¹¹ while recent approaches to dissociation have focused on L^2 continuum discretization techniques.¹²

In this paper we present a rotating-frame transformation which provides a new and powerful way of approaching the evaluation of the time evolution of a many-level system in the presence of an intense coherent field. Starting with the equations of motion in the conventional interaction representation, the system is transformed with a novel unitary rotating-frame transformation to yield a separation of time-independent from time-dependent terms in the Hamiltonian. The transformation is chosen such that the former contain essentially all of the information pertaining to the most nearly resonant multiphoton transitions from the ground state to all other states. Neglect of the time-dependent terms gives an equation of motion with only time-independent interactions which is readily solved for the distribution of molecular-state populations as a function of time. The tridiagonal rotating-wave approximation is seen to result from a particularly

simple choice of the rotating-frame transformation. The great advantage of our general rotating-frame transformation is that it is molecule and field specific, i.e., it can be chosen to partially compensate for the effects of anharmonicities and for variations in the transition matrix elements at any given point in the molecular-level structure. It provides explicit construction of a time-independent interaction matrix containing the bulk of the information relevant to the multiphoton excitation process. For a given molecular-level system, the molecule-field energies and couplings most relevant to multiphoton absorption at a particular laser frequency are deposited in the time-independent matrix. There is also no restriction to a single laser field. The transformation can in principle equally well be defined for a multilevel system interacting with several laser fields. There is, however, a restriction to one molecule-field state per molecular state.

We demonstrate the power of this rotating-frame transformation by applying it to the multiphoton excitation and dissociation dynamics of a Morse oscillator, utilizing the same parameters (appropriate to the C—H bond) as those of Schek, Jortner, and Sage.¹⁰ The results obtained on neglect of all time-dependent terms after transformation are seen to be essentially equivalent to the full time-dependent calculation of Schek *et al.* who use the Magnus expansion to third order and multiple-time intervals.¹⁰ The importance of such a transformation lies then in its ability to include the couplings relevant to the multiphoton process in a time-independent approximate Hamiltonian which is simple to solve for the time evolution of the molecular system. Although our example here is for a diatomic molecule, the method is not restricted to one dimension. As long as a molecular-level structure can be explicitly given, a rotating-frame transformation which essentially selects pathways of absorption may be defined. It is, therefore, appropriate for the description of excitation into and possibly also within the quasicontinuum of large polyatomic molecules, and for multiphoton absorption over the entire level structure of small polyatomic molecules.

Before presenting the rotating-frame transformation, we discuss previous generalizations of the rotating-wave approximation to a many-level system in Sec. II. A clear understanding of the meaning of the rotating-wave approximation will be necessary for what follows. The rotating-frame transformation is presented in Sec. III, and solution of the resulting time-independent approximate Hamiltonian (which is, in general, non-Hermitian for dissociative systems) is given in Sec. IV. Since we are concerned with the multiphoton excitation of an isolated molecule in collision-free conditions, we use the Schrödinger wave equation rather than the density-matrix approach throughout this paper. We shall also, for simplicity, take multilevel systems to refer to molecular-level systems, and consider the radiation field to be laser radiation, although the treatment is quite general. Section V contains the results for the time evolution of a dissociative Morse oscillator and a comparison of these results with the exact time-dependent calculation of Schek *et al.*¹⁰ Finally, in Sec. VI we summarize and discuss implications of the transformation.

II. ROTATING-WAVE APPROXIMATION FOR MANY-LEVEL SYSTEMS

As originally applied to a two-level system in the presence of a near resonant oscillating electromagnetic field, there are two conditions required for validity of the RWA. The first is that the field frequency be much larger than the energy defect, and the second is that the field frequency exceed the Rabi frequency, defined as $\mu_{01}E/2\hbar$, with μ_{01} the transition dipole moment and E the electric field strength. To be explicit, we briefly review the two-level system here. (Throughout this paper we shall use the semiclassical formalism for radiation-matter interactions. In the absence of spontaneous emission this gives equivalent results to the fully quantized form.)

The wave function for a two-level system is written in the interaction representation as

$$\psi(\{r\}, t) = b_0(t)e^{-i\omega_0 t}\phi_0(\{r\}) + b_1(t)e^{-i\omega_1 t}\phi_1(\{r\}), \quad (1)$$

where $\{r\}$ refers to the collective spatial and/or spin coordinates of the system and the energy eigenvalues are E_i , with

$$\omega_i = E_i / \hbar. \quad (2)$$

In the dipole approximation, the semiclassical Hamiltonian for interaction with a linearly polarized monochromatic electromagnetic field is

$$H = H_0 + \vec{\mu} \cdot \vec{\epsilon} E \cos(\omega t), \quad (3)$$

where H_0 is the molecular Hamiltonian, $\vec{\mu}$ the dipole moment operator, and $\vec{\epsilon}$ the (real) polarization vector. The time-dependent Schrödinger equation for the amplitudes $b_i(t)$ is then

$$i\dot{\vec{b}}(t) = \begin{bmatrix} 0 & D_{01}e^{i(\omega_{01}+\omega)t} \\ D_{10}e^{i(\omega_{10}-\omega)t} & 0 \end{bmatrix} \vec{b}(t) + \begin{bmatrix} 0 & D_{01}e^{i(\omega_{01}-\omega)t} \\ D_{10}e^{i(\omega_{10}+\omega)t} & 0 \end{bmatrix} \vec{b}(t) \quad (4)$$

$$= [\underline{M}(t) + \underline{M}'(t)] \vec{b}(t), \quad (5)$$

where

$$\omega_{ij} = \omega_i - \omega_j \quad (6a)$$

and

$$D_{ij} = \frac{1}{2}\mu_{ij}E/\hbar = \frac{1}{2}\langle \phi_i | \vec{\mu} \cdot \vec{\epsilon} | \phi_j \rangle E / \hbar, \quad (6b)$$

and we have assumed that $\mu_{ii} = 0$ for $i = 0, 1$.

The RWA is now made by neglecting the second matrix $\underline{M}'(t)$. This amounts to replacing the oscillating field $\vec{\epsilon}E \cos(\omega t)$ by a rotating (circularly polarized) field, $\vec{\epsilon}E e^{i\omega t}$. For a two-level system, the resulting equations for $\vec{b}(t)$ can then be solved analytically. The RWA is justified on the grounds that for frequencies near resonance with ω_{01} , the matrix elements of $\underline{M}'(t)$ oscillate much faster than corresponding elements of $\underline{M}(t)$. So the integrated contribution of these elements averages to zero on a time scale over which $\underline{M}(t)$ shows little variation. It is clear from direct integration of (4) that for the RWA to be valid one requires that

$$\omega \gg |\omega_{10} - \omega| \quad (7)$$

and

$$\omega \gg |\mu_{01}E/(2\hbar)| = |D_{01}|. \quad (8)$$

The effect of the antiresonant matrix $\underline{M}'(t)$ is well known, and introduces intensity-dependent shifts of the molecular levels (Bloch-Siegert shifts).

In the extension of Eq. (5) to an N -level system in the presence of a single-laser frequency ω , matrices $\underline{M}(t)$ and $\underline{M}'(t)$ become

$$\underline{M}(t) = \begin{bmatrix} 0 & D_{01}e^{i(\omega_{01}+\omega)t} & D_{02}e^{i(\omega_{02}+\omega)t} & \cdots & D_{0,N-1}e^{i(\omega_{0,N-1}+\omega)t} \\ D_{10}e^{i(\omega_{10}-\omega)t} & 0 & D_{12}e^{i(\omega_{12}+\omega)t} & \cdots & D_{1,N-1}e^{i(\omega_{1,N-1}+\omega)t} \\ D_{20}e^{i(\omega_{20}-\omega)t} & D_{21}e^{i(\omega_{21}-\omega)t} & 0 & \cdots & D_{2,N-1}e^{i(\omega_{2,N-1}+\omega)t} \\ \vdots & \vdots & \vdots & \vdots & \vdots \\ \cdots & \cdots & \cdots & 0 & \cdots \\ D_{N-1,0}e^{i(\omega_{N-1,0}-\omega)t} & D_{N-1,1}e^{i(\omega_{N-1,1}-\omega)t} & D_{N-1,2}e^{i(\omega_{N-1,2}-\omega)t} & D_{N-1,N-2}e^{i(\omega_{N-1,N-2}-\omega)t} & 0 \end{bmatrix} \quad (9)$$

$$= \underline{M}(\omega, t)$$

and

$$\underline{M}'(t) = \underline{M}(-\omega, t), \quad (10)$$

where ω_{ij} is defined as before [Eqs. (2) and (6a)] and we similarly set $\mu_{ii} = 0$ for all i . Thus $\underline{M}(t)$ contains the terms in which the molecular phasors $e^{\pm i|\omega_{ij}|t}$ rotate in an opposite direction to the field phasors $e^{\mp i|\omega|t}$, while $\underline{M}'(t)$ contains the terms in which they rotate in the same sense. Since for positive ω , terms in $\underline{M}(t)$ are always more slowly varying than corresponding terms in $\underline{M}'(t)$ (unless some energy levels are degenerate), we shall continue to refer to $\underline{M}'(t)$ as the antiresonant matrix and refer to $\underline{M}(t)$ as the proresonant matrix in the interaction representation. The generalization to several frequencies, $\omega^{(f)}$, is obvious, with each term in $\underline{M}(t)$ and $\underline{M}'(t)$ being replaced by a sum of terms, one for each frequency $\omega^{(f)}$.

Generalization of the rotating-wave approximation to many-level systems has been considered by several authors in recent years.⁸⁻¹⁰ A formal generalization for a system in the presence of multiple laser frequencies $\omega^{(f)}$ was made by Einwohner, Wong, and Garrison⁸ in which the entire antiresonant matrix $\underline{M}'(t)$ and also all terms in $\underline{M}(t)$ containing field frequencies not close to resonance were neglected. A frequency $\omega^{(f)}$ is said to be close to resonance for a transition between levels i and j if

$$| |\omega_{ij}| - \omega^{(f)} | \leq \lambda \bar{\omega}, \quad (11)$$

where $\bar{\omega}$ is a typical frequency and $\lambda = O(\mu_{ij}E/\bar{\omega})$. This condition is somewhat more restrictive than that of Eqs. (7) and (8). With this in mind we propose to refer to the approximation made by neglecting the antiresonant matrix $\underline{M}'(t)$ as the global rotating-wave approximation and to the further approximation of Einwohner *et al.* as the resonance constrained global RWA. After making this resonance constrained global RWA, the authors employ a variable unitary transformation to eliminate time dependence in the remainder of the proresonant matrix $\underline{M}(t)$. Using graph theory they examine the conditions under which all the remaining time dependence can be consistently eliminated. In essence this transformation is very similar to the rotating-frame transformation introduced in the next section, but as we shall see, the absence of a near resonance constraint such as Eq. (11) will grant considerably more flexibility. Our treatment of the rotating-frame transformation also leads to *explicit* construction of the time-independent interaction matrix for radiation of a given frequency incident upon a particular multilevel system.

For certain special classes of matrix elements and energy defects $|\omega_{ij}| - \omega^{(f)}$ the resulting eigenvalue problem can be solved analytically for N -level and infinite-level systems. In particular, extensive studies have been performed on the tridiagonal system of equations obtained by retaining only coupling between adjacent energy levels in $\underline{M}(t)$.⁹ In this case a unitary transformation which eliminates time dependence in all off-diagonal elements of $\underline{M}(t)$ can always be defined. Because of its importance in previous work^{2,9,10} we refer to this as the tridiagonal RWA, whether or not the near resonance constraint, Eq. (11), is added. When the resonance constraint is enforced, it implies either the presence of many laser frequencies for

anharmonic systems, or, for a monochromatic laser field, excitation of a harmonic level sequence.

The resonance constrained RWA systems were illuminating for the information they shed on population inversion from coherent excitation, but the physical models to which the analytically soluble examples correspond are highly restrictive. For realistic molecular systems, even for the simplest diatomic models, it will be necessary to solve eigenvalue problems which have no explicit analytic solutions. A more serious concern is the stringent requirements imposed by the near resonance constraint, Eq. (11). Molecular transitions are only included in the interaction matrix if they are close to some laser frequency. Thus the resonance constrained global RWA is not appropriate for description of the multiphoton excitation of strongly anharmonic systems by monochromatic laser radiation. We shall see in the next section how a representation may be obtained in which the couplings and energy defects relevant to the multiphoton excitation of such systems may be included in the time-independent portion of the interaction matrix without making such a restriction. This will also show significant improvement over the tridiagonal RWA, which is only valid for describing excitation of systems which are nearly harmonic (e.g., the lowest, sparsely populated energy region of polyatomic molecules in single-mode vibrational excitation with an infrared laser). The tridiagonal RWA breaks down at higher levels of anharmonic systems where the generalization of Eq. (7), namely

$$\omega \gg | |\omega_{ij}| - \omega | \quad (12)$$

is no longer valid.¹⁰

III. ROTATING-FRAME TRANSFORMATION FOR COHERENT MULTIPHOTON PROCESSES

Consider a discrete N -level system such as a sparse set of molecular-energy levels, in the presence of monochromatic laser radiation. Generalization to several frequencies will be briefly discussed later. Since we are concerned with multiphoton excitation, the laser frequency ω is assumed to be of the same order of magnitude as the lowest energy spacing ω_{01} , though not necessarily near resonant with this. Dissociation will be simulated by the addition of a phenomenological decay width Γ to the energy of the highest state. With $\Gamma = 0$ one then regains the case of coherent excitation in a multilevel bound system.

The Hamiltonian is given by Eq. (3), with H_0 the molecular Hamiltonian having eigenvalues $E_0, E_1, \dots, E_{N-2}, E_{N-1} - i\Gamma_{N-1}\hbar$. The molecular wave function

$$\psi(\{r\}, t) = \sum_{j=0}^{N-1} a_j(t) \phi_j(\{r\}) \quad (13)$$

is written as before in an interaction representation in which the phase is determined by the real parts of the eigenvalues,

$$\psi(\{r\}, t) = \sum_{j=0}^{N-1} b_j(t) e^{-iE_j t/\hbar} \phi_j(\{r\}). \quad (14)$$

In this representation the time-dependent Schrödinger

$$\underline{P}(t) = \begin{pmatrix} 0 & 0 & D_{02}e^{-i\omega t} & D_{03}e^{-2i\omega t} & \dots & \dots & \dots \\ 0 & 0 & 0 & D_{13}e^{-i\omega t} & \dots & \dots & \dots \\ D_{20}e^{+i\omega t} & 0 & 0 & 0 & \dots & \dots & \dots \\ D_{30}e^{+2i\omega t} & D_{31}e^{+i\omega t} & 0 & 0 & \dots & \dots & \dots \\ \vdots & \vdots & \vdots & \vdots & \vdots & \vdots & \vdots \\ \vdots & \vdots & \vdots & \vdots & 0 & 0 & D_{N-3,N-1}e^{-i\omega t} \\ \dots & 0 & 0 & 0 & \dots & \dots & \dots \\ \dots & D_{N-1,N-3}e^{+i\omega t} & 0 & 0 & \dots & \dots & \dots \end{pmatrix} \quad (25a)$$

and

$$[\underline{P}'(t)]_{jk} = \begin{cases} [\underline{P}(t)]_{jk}e^{-2i\omega t}, & k > j+1 \\ D_{jk}e^{-2i\omega t}, & k = j+1 \\ 0, & k = j \end{cases} \quad (25b)$$

$$[\underline{P}'(t)]_{jk} = [\underline{P}'(t)]_{kj}^*, \quad k < j.$$

The exponents no longer contain any molecular frequencies but the phase velocity difference of 2ω between corresponding elements in $\underline{M}(t)$ and $\underline{M}'(t)$ has been preserved.

As the molecular spacings decrease at high energies the accuracy of the tridiagonal RWA breaks down and couplings between nonadjacent states become significant. It is then no longer valid to neglect $\underline{P}(t)$ in the above representation. [However, in the tridiagonal representation the elements of $\underline{P}'(t)$ all oscillate at a rate 2ω faster than the elements of $\underline{P}(t)$ and so can be either uniformly neglected or included. The relative importance of $\underline{P}'(t)$ increases only with laser intensity.] When the equations of motion (15) or (18) are solved exactly, with the use of the Magnus expansion, for the simple example of a dissociative Morse oscillator, it is found necessary to include up to third-order terms in the Magnus expansion in order to ensure convergence.¹⁰ The Magnus expansion for the time-evolution operator (see Appendix) involves successively higher dimensional integrals over multiple commutators of the time-dependent Hamiltonian, $\underline{N} + \underline{P}(t) + \underline{P}'(t)$. It is shown in the Appendix that the presence of increasingly large energy defects Δ_{j0} along the principal diagonal in \underline{N} causes slow convergence. Thus the exact solution of the time-dependent equations is very tedious and time (CPU) consuming.

B. General RFT

We can circumvent the problem by redefining the rotating-frame transformation e^{iqt} to minimize the absolute value of the real parts of the diagonal elements in \underline{N} , i.e., $|q_j|$. These are defined sequentially as before, starting with $q_0 = 0$, but for general j we now define

$$q_j = m_j\omega - \omega_{j0} \quad (26)$$

with m_j an integer such that $|q_j| < \omega/2$. Substituting this into (23) then gives the condition that δ_{jk} vanishes when

$$m_j - m_k = -1 \quad \text{and} \quad j < k \quad (27a)$$

or when

$$m_k - m_j = -1 \quad \text{and} \quad j > k. \quad (27b)$$

The resulting time-independent interaction matrix \underline{N} is a sparsely populated matrix which is only tridiagonal for near harmonic systems. The form of this matrix is better understood by rewriting Eq. (26) as

$$q_j = (j - n_j)\omega - \omega_{j0}. \quad (28)$$

Then for ω near resonant with ω_{01} , $n_j = 0$ when the system is nearly harmonic and (28) reduces to (21). For the example of a Morse oscillator (Sec. IV) this will be true for small j . As j increases, n_j increases monotonically so that Eqs. (27) can be satisfied between pairs of states other than $j = k \pm 1$ and couplings between nonadjacent molecular states are thereby put into \underline{N} . Also, whenever n_j increases by unity, a given value of n_j may satisfy Eqs. (27) for more than one value of k . In this case several pairs of matrix elements D_{jk} and D_{kj} will appear in \underline{N} , introducing extra couplings into \underline{N} relative to those achieved by the tridiagonal transformation.

As a simple example, consider the sequence $j = 5-9$ with

$$\begin{aligned} q_5 &= 5\omega - \omega_{50}, \\ q_6 &= 6\omega - \omega_{60}, \\ q_7 &= 7\omega - \omega_{70}, \\ q_8 &= 7\omega - \omega_{80}, \\ q_9 &= 8\omega - \omega_{90}, \end{aligned} \quad (29)$$

corresponding to a gradual increase in anharmonicity sufficient to cause n_j to increase from 0 to 1 for $j = 8$. The appropriate choice of q_9 will eliminate time dependence in two pairs of matrix elements of $e^{iqt}\underline{M}^D(t)e^{-iqt}$, $(i,j) = (8,9)$ and $(9,8)$ as well as $(7,9)$ and $(9,7)$. The tridiagonal transformation puts only D_{89} and D_{98} into \underline{N} . For a highly anharmonic system such as a Morse oscillator, the resulting interaction matrix $\underline{N}^{\text{RFT}}$ will contain an extensive number of off-diagonal terms, corresponding to additional possible near resonant pathways for multiphoton absorption.

A slight ambiguity arises when $|q_j| = \omega/2$ for some j , since then there are two possible values of m_j . This will give rise to small local changes in the matrix \underline{N} and will

with the initial state can be accessed via sequential one-photon or simultaneous multiphoton absorption from this initial state.

A diagrammatic representation of this is given in Fig. 1 for an anharmonic sequence of molecular energy levels $j=0,1,\dots,7$ and a single frequency $\omega \lesssim \omega_{10}$. The photon number m_j decreases from left to right. The vertical position of a level gives its total molecule-field energy, $E_j + (\mathcal{N} - m_j)\omega$. The levels with energies in the range $E_0 + \mathcal{N}\omega \pm \frac{1}{2}\omega$ are indicated by thick solid lines and are labeled explicitly. One-photon couplings between this subset of eight states are drawn as dotted lines. This clearly illustrates the origin of the extra couplings in $\underline{N}^{\text{RFT}}$ as additional one-photon pathways of absorption.

D. Effect of initial conditions on the RFT

The discussion in the preceding section suggests that the general RFT as defined in Eq. (26) will be very appropriate for absorption from the ground state, $j=0$, but this specific transformation with $q_0=0$ may not give a good representation for initial conditions corresponding to higher molecular states, $j>0$. In such a situation we can generalize Eq. (26) by setting $q_j=0$ where $j=J$ is the initial state and then defining

$$q_j = m_j\omega - \omega_{jJ} \quad (36a)$$

$$= m_j\omega - E_j + E_J, \quad (36b)$$

with the same condition on m_j , namely m_j an integer such that $|q_j| < \omega/2$. This gives the same form of matrix \underline{N} , with couplings included according to Eqs. (27) as before, but with m_j now negative for $j < J$. Comparison of Eqs. (31) and (36) show that we have now effectively chosen the

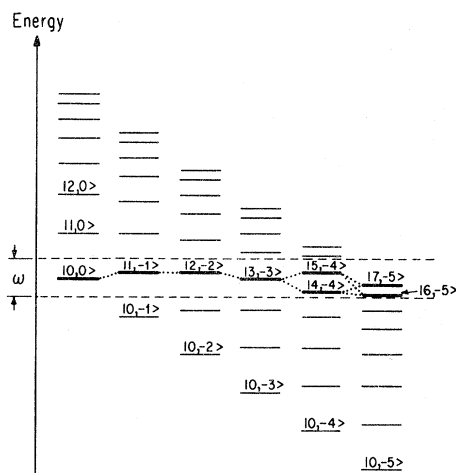


FIG. 1. Energy-level scheme for the fully quantized molecule-field states of an anharmonic molecular system with a single laser frequency ω , showing the effect of the RFT. Molecule-field states are denoted by $|j-m_j\rangle$ where j is the molecular state index and m_j is the photon number (see text). Thick solid lines refer to the levels within the energy range $\pm\omega/2$ about the initial state $|0,0\rangle$. One-photon couplings between this subset of states are indicated as dotted lines. These couplings form the off-diagonal elements of the time-independent interaction matrix $\underline{N}^{\text{RFT}}$ in the semiclassical limit.

set of molecule-field states closest to resonance with the specific initial state $|J,0\rangle$. Thus in Eq. (32), $E_{0\perp}$ will be replaced by $E_{J\perp}$.

E. Time-dependent matrices $\underline{P}(t)$ and $\underline{P}'(t)$

The variable RFT maintains the phase velocity difference of 2ω between corresponding matrix elements in $\underline{P}(t)$ and $\underline{P}'(t)$ and again, just as with the tridiagonal transformation, no molecular frequencies occur in these matrices. However, it may now happen that the corresponding terms oscillate at equal rates, i.e., when $[\underline{P}]_{jk}(t) = D_{jk}e^{+i\omega t}$ and $[\underline{P}']_{jk}(t) = D_{jk}e^{-i\omega t}$ ($j < k$). This is illustrated in the simple example of Eqs. (29) where $P_{78}(t) = D_{78}e^{+i\omega t}$ and $P'_{78}(t) = D_{78}e^{-i\omega t}$. For these terms and also for couplings at very high anharmonicities when $\omega_{ij} \sim 0$ so that

$$|\omega_{ij}| + \omega \sim -(|\omega_{ij}| - \omega), \quad (37)$$

it would not be valid to neglect the antiresonant matrix $\underline{P}'(t)$ relative to the proresonant matrix $\underline{P}(t)$, and the global RWA may not be valid. However, in general, the number of these terms will be small and their importance limited. We shall see in Sec. V that at least for the example of multiphoton excitation of a Morse oscillator, these terms appear to have little effect on the overall excitation dynamics. The matrix $\underline{P}'(t)$ can be assumed to be important only at very high intensities, when it gives rise to intensity dependent shifts of the molecular energy levels.

The crucial point concerning the approximation made by neglecting $\underline{P}(t)$ and $\underline{P}'(t)$ is that after transformation with the variable RFT, the diagonal terms are minimized in the time-independent interaction matrix \underline{N} . This will decrease the size of higher-order commutators in the Magnus expansion and improve convergence, to the extent that the first term only may be sufficient. This is then equivalent to solving the eigenvalue problem, Eq. (19). A small variation in effectiveness of this approximation as a function of ω may be expected, since the range in size of the diagonal elements increases with ω [Eq. (26)].

F. Extension to interactions with several laser frequencies

When the radiation field contains several frequencies, each term in the time-dependent matrices $\underline{M}^D(t)$ and $\underline{M}'(t)$ in the interaction representation becomes a sum of terms containing one component for each laser frequency $\omega^{(f)}$. Thus for n different frequencies we have

$$[\underline{M}^D(t)]_{jk} = \sum_{f=1}^n D_{jk}^{(f)} e^{i(\omega_{jk} + \omega^{(f)})t}, \quad (38a)$$

$$[\underline{M}'(t)]_{jk} = \sum_{f=1}^n D_{jk}^{(f)} e^{i(\omega_{jk} - \omega^{(f)})t}, \quad (38b)$$

where $D_{jk}^{(f)} = \mu_{ij} E^{(f)} / 2\hbar$, with $E^{(f)}$ the electric field strength of the frequency component $\omega^{(f)}$.

A rotating-frame transformation e^{iqt} specified by N diagonal elements $e^{iq_j t}$ will be able to eliminate the time dependence of at most one term in the sum for each matrix element of $\underline{M}^D(t)$. There are various ways of generalizing the near resonance criterion for choosing q_j , Eq.

(26). Defining q_j in terms only of the laser frequencies $\omega^{(f)}$ and the molecular frequencies ω_{jk} , as before, will again allow an interpretation in terms of selecting a finite subset of molecule field states from the now multiply infinite set of fully quantized states. A little reflection then shows that sequential definition of q_j is essential to guarantee a continuously connected time-independent interaction matrix \underline{N} , and hence excitation of the entire molecular-level structure from a pure initial state in the time-independent approximation, Eq. (19). Assuming for simplicity that the initial molecular state is the ground state, one defines

$$q_0 = 0 \quad (39a)$$

and

$$q_1 = \omega^{(f_1)} - \omega_{10}, \quad (39b)$$

where $\omega^{(f_1)}$ gives the best, i.e., minimum value of $|q_1|$. Now q_2 is defined as

$$q_2 = q_1 + n_2^{(f_2)} \omega^{(f_2)} - \omega_{21}, \quad (40)$$

with $n_2^{(f_2)}$ equal to zero or one such that $|q_2| < \omega^{(F)}/2$ and $\omega^{(f_2)}$ such that this value of $|q_2|$ is minimized. (The first condition requires that the maximum separation of a given molecular energy level from the lower levels does not exceed $3\omega^{(F)}/2$, where $\omega^{(F)}$ is the maximum laser frequency present.)

Proceeding in this manner one finds that as long as $n_j^{(f_j)}$ is equal to zero or one, the levels will be continuously connected, avoiding the problem of forming disconnected blocks in the time-independent interaction matrix \underline{N} . The time-independent couplings now arise from different time-dependent terms $D_{jk}^{(f)}$ in $\underline{M}(t)$, according to which frequency $\omega^{(f)}$ is added to q_j at each stage in \underline{q} . Let the sum over l of all terms $n_l^{(f_l)} \omega^{(f_l)}$ in q_j be denoted by $\bar{m}_j(\{\omega^{(f)}\})$. Then we may rewrite q_j as

$$q_j = \bar{m}_j(\{\omega^{(f)}\}) \quad (41a)$$

$$= n_1^{(f_1)} \omega^{(f_1)} + n_2^{(f_2)} \omega^{(f_2)} + n_3^{(f_3)} \omega^{(f_3)} + \cdots + n_j^{(f_j)} \omega^{(f_j)} - \omega_{j0}. \quad (41b)$$

In the fully quantized representation the molecule-field state $|j, -\bar{m}_j\rangle$ isomorphic to ϕ_j is now related to the initial state $|0,0\rangle$ by absorption of several photons of different frequencies. For a given frequency $\omega^{(f)}$, the sum of all $n_l^{(f_l)}$ in q_j for which $f_l = f$ represents the total number of photons of that frequency which have been absorbed to get from $|0,0\rangle$ to $|j, -\bar{m}_j\rangle$.

Two levels j and k are connected in \underline{N} by $D_{jk}^{(f)}$ (and $D_{kj}^{(f)}$) if

$$q_j - q_k + \omega_{jk} + \omega^{(f)} = 0. \quad (42)$$

Now since $\bar{m}_j(\{\omega^{(f)}\})$ is contained in $\bar{m}_k(\{\omega^{(f)}\})$ for all $j < k$ and n_j is at most one, there will always be some $j < k$ for which

$$\bar{m}_j(\{\omega^{(f)}\}) - \bar{m}_k(\{\omega^{(f)}\}) = -\omega^{(i)} \quad (43)$$

causing $D_{jk}^{(i)}$ to appear in \underline{N} . Thus \underline{N} is a continuously connected matrix. This is illustrated in Table I for a simple eight-level system.

In the particular case when there is one (and only one) frequency close to resonance with each molecular transition [according to the closeness criterion of Eq. (11)], the structure of the time-independent matrix \underline{N} is equivalent to the acyclic graphs of Einwohner, Wong, and Garrison.⁸ However, the above choice of \underline{q} has now eliminated the element of arbitrariness in the phase of the transformation e^{iqt} and furthermore allowed the useful analogy to the fully quantized formalism to be drawn.

The variation in compensating frequency $\omega^{(f)}$ for each j causes the couplings in \underline{N} to contain variable intensity, according to which particular term $D_{jk}^{(f)}$ in the sum from matrix elements $[\underline{M}^D(t)]_{jk}$ they were derived. Both this choice of \underline{q} for the many-frequency system and that for the single-frequency case are clearly chosen according to resonance criteria only. Large intensity differences between the various frequency components $\omega^{(f)}$ may require local modification of the transformation e^{iqt} . For instance, one frequency $\omega^{(i)}$ may minimize $|q_j|$ for some j , giving rise to coupling $D_{jk}^{(i)}$ in \underline{N} , but the intensity factor $E^{(i)}$ makes the transition $k \rightarrow j$ via $\omega^{(i)}$ far less favorable than via some other frequency $\omega^{(i')}$ for which the resulting $|q_j|$ is larger.

TABLE I. Example of the general RFT for a model eight-level system, $j=0,1,\dots,7$ in the presence of three laser frequencies. The frequencies are $\omega^{(1)}=0.9$, $\omega^{(2)}=0.4$, and $\omega^{(3)}=0.3$, in arbitrary units. Energy levels E_j are given in the same units. The quantities q_j and $D_{ij}^{(f)}$ constitute the diagonal and off-diagonal elements of \underline{N} , respectively (see text).

j	E_j	q_j	Couplings brought into \underline{N} from $\underline{M}(t)$
0	0	0	0
1	1	$\omega^{(1)} - \omega_{10}$	$D_{01}^{(1)}, D_{10}^{(1)}$
2	2	$2\omega^{(1)} - \omega_{20}$	$D_{12}^{(1)}, D_{21}^{(1)}$
3	2.2	$2\omega^{(1)} + \omega^{(2)} - \omega_{30}$	$D_{23}^{(2)}, D_{32}^{(2)}$
4	2.4	$2\omega^{(1)} + \omega^{(2)} + \omega^{(3)} - \omega_{40}$	$D_{34}^{(3)}, D_{43}^{(3)}$
5	2.9	$2\omega^{(1)} + 2\omega^{(2)} + \omega^{(3)} - \omega_{50}$	$D_{45}^{(2)}, D_{54}^{(2)}$
6	3.0	$2\omega^{(1)} + 2\omega^{(2)} + \omega^{(3)} - \omega_{60}$	$D_{46}^{(2)}, D_{64}^{(2)}$
7	3.8	$3\omega^{(1)} + 2\omega^{(2)} + \omega^{(3)} - \omega_{70}$	$D_{57}^{(1)}, D_{75}^{(1)}, D_{67}^{(1)}, D_{76}^{(1)}$

IV. TIME EVOLUTION OF A DISSOCIATIVE SYSTEM IN THE ROTATING-FRAME APPROXIMATION

Since \underline{N} is a symmetric matrix, the solution of Eq. (19) is formally very similar for both nondissociative ($\Gamma=0$) and dissociative ($\Gamma\neq 0$) systems, despite the fact that \underline{N} is non-Hermitian in the latter case. A complex symmetric matrix may always be diagonalized by an orthogonal transformation.¹⁵ Thus

$$\underline{T}^T \underline{N} \underline{T} = \underline{\lambda}, \quad (44)$$

where

$$\underline{T} \underline{T}^T = \underline{1} \quad (45)$$

and $\underline{\lambda}$ is the diagonal matrix of eigenvalues. This yields the solution to Eq. (19) in the rotating-frame basis

$$\underline{\bar{c}}(t) = \underline{T} e^{-i\lambda(t-t_0)} \underline{T}^T \underline{\bar{c}}(t_0) \quad (46)$$

and the time evolution of the original molecular amplitudes $\bar{a}(t)$ is then given by back transformation using Eqs. (13), (14), and (16):

$$\bar{a}(t) = e^{-iEt} e^{-iqt} \underline{T} e^{-i\lambda(t-t_0)} \underline{T}^T e^{iqt_0} e^{iEt_0} \bar{a}(t_0). \quad (47)$$

The matrix \underline{T} is real when $\Gamma=0$ and complex when $\Gamma\neq 0$. The matrix solution, Eq. (47), is thus formally identical for Hermitian and non-Hermitian \underline{N} but since the eigenvectors of a non-Hermitian matrix are not in general orthogonal, there is a difference which is apparent when Eq. (45) is written in bracket notation. Without loss of generality, let \underline{T} be the matrix of normalized eigenvectors of \underline{N} , i.e., the columns of \underline{T} are formed by the eigenvectors $|\psi_k\rangle$ of \underline{N} . Denoting the matrix \underline{T} by $|\underline{\psi}\rangle$ and \underline{T}^T by $\langle\underline{\psi}|$, Eq. (45) becomes

$$|\underline{\psi}\rangle \langle\underline{\psi}| = \underline{1}, \quad (48)$$

which is the generalization of the closure relation to non-Hermitian operators, and identifies $|\underline{\psi}\rangle$ as the set of vectors orthogonal to $|\underline{\psi}\rangle$. Using the definition of the bra as the (Hermitian) adjoint of a ket, this implies

$$|\underline{\psi}\rangle = \langle\underline{\psi}|^\dagger \quad (49a)$$

$$= \underline{T}^* \quad (49b)$$

When \underline{T} is real, the vectors $|\underline{\psi}\rangle$ become equal to eigenvectors $|\psi\rangle$, as required by the orthogonality of eigenvectors of a Hermitian operator. For complex \underline{T} , $|\underline{\psi}\rangle$ is the set of eigenvectors of \underline{N}^\dagger , the Hermitian adjoint of \underline{N} . It is important to note that the normalization of the eigenvectors $|\underline{\psi}\rangle$ is then defined by the adjoint of Eqs. (45) and (48), namely by

$$\underline{T}^T \underline{T} = \underline{1} \quad (50)$$

rather than the usual normalization for eigenvectors of Hermitian operators

$$\begin{aligned} \underline{T}^\dagger \underline{T} &= (\underline{T}^T)^* \underline{T} \\ &= \underline{1}. \end{aligned} \quad (51)$$

The properties of non-Hermitian Hamiltonians are dis-

cussed more fully in Ref. 16.

The general rotating-frame transformation, Eq. (26), and approximation, Eq. (19), were applied to the multi-photon excitation of the vibrational manifold of an isolated diatomic molecule, simulated by a Morse oscillator. The bound energy levels are given by

$$E_j = -D \left[1 - (j + \frac{1}{2}) \frac{\alpha \hbar}{(2mD)^{1/2}} \right]^2 \quad (52)$$

for $j=0, 1, 2, \dots, N-1$. D is the well depth, α the range parameter, and m the reduced mass. The number of bound states N is the closest integer from below to $(C + \frac{1}{2})$, where $C^{-1} = \alpha \hbar / (2mD)^{1/2}$. An equivalent expression for the energy levels is

$$\begin{aligned} E_j &= -D + \omega_e(j + \frac{1}{2}) - X(j + \frac{1}{2})^2 \\ &= -D_0 + \omega_0 j - Xj^2, \\ D_0 &= D - \frac{1}{2}\omega_e + \frac{1}{4}X \end{aligned} \quad (53)$$

where the ground-state frequency is $\omega_e = (2D/m)^{1/2} \alpha \hbar$ and the anharmonicity constant is $X = \alpha^2 \hbar^2 / 2m$. The uppermost state is assigned a (rotationally) predissociative decay width, which, following Schek *et al.*¹⁰ was parametrized as $\Gamma = X/20$. The functional form of the dipole moment operator $\mu(r)$ was also taken from Schek *et al.*¹⁰ The coordinate r is the internuclear distance. Two forms of $\mu(r)$ were used: (i) the linear dipole function $\mu(r) = kr$, and (ii) the exponential dipole function $\mu(r) = kr \exp(-r/r^*)$. Here r^* is a constant related to the equilibrium distance r_0 and k a constant which does not need to be specified when the laser power is expressed in terms of the first Rabi frequency,

$$\begin{aligned} \omega_R &= D_{01} \\ &= \mu_{01} E / 2\hbar. \end{aligned} \quad (54)$$

The quantities of interest in assessing the accuracy of the approximation, Eq. (19), are the molecular-state populations, $|a_j(t)|^2$ and the probability of dissociation $P_D(t)$ as functions of time. The molecular system is assumed to be in the ground state before the radiation field is switched on at $t=0$, i.e., $a_j(0) = \delta_{j0}$. Then from Eq. (47)

$$|a_j(t)|^2 = \sum_{k,k'} T_{jk} T_{jk'}^* e^{-i(\lambda_k - \lambda_{k'})t} T_{0k} T_{0k'}^*. \quad (55)$$

For a system with a finite number of bound levels, the dissociation probability $P_D(t)$ is simply given by

$$P_D(t) = 1 - \sum_{j=0}^{N-1} |a_j(t)|^2. \quad (56)$$

We are not concerned here with contributions to dissociation after the laser field is switched off. Thus t is by implication a time smaller than or equal to a typical laser pulse length. The average energy absorbed by the molecule may be derived from $|a_j(t)|^2$ and $P_D(t)$:

$$E_{av} = \sum_{j=0}^{N-1} E_j |a_j(t)|^2 + E_{N-1} P_D(t). \quad (57)$$

The identification of the uppermost state $j=N-1$ as a metastable state provides an alternative form of $P_D(t)$ which is computationally simpler and leads to a useful approximation. The decay rate of a normalized metastable state with complex energy $\tilde{E}_{N-1} = E_{N-1} - i\Gamma_{N-1}$ is given by $2\Gamma_{N-1} |a_{N-1}(t)|^2$. Since dissociation can only occur via decay from the $N-1$ molecular level, we have

$$P_D(t) = 2\Gamma_{N-1} \int_0^t |a_{N-1}(t')|^2 dt'. \quad (58)$$

Diagonalization of \underline{N} causes the imaginary term $-i\Gamma_{N-1}$

$$P_D(t) = 2\Gamma_{N-1} \sum_k \int_0^t |f_k^{N-1}|^2 e^{-2\gamma_k t'} dt' + 2\Gamma_{N-1} \sum_{\substack{k,k' \\ k \neq k'}} \int_0^t f_k^{N-1} f_{k'}^{N-1*} e^{-i(\lambda_k - \lambda_{k'}^*)t'} dt' \quad (61)$$

$$= \Gamma_{N-1} \sum_k |f_k^{N-1}|^2 \left[\frac{1 - e^{-2\gamma_k t}}{\gamma_k} \right] + 2\Gamma_{N-1} \sum_{\substack{k,k' \\ k \neq k'}} f_k^{N-1} f_{k'}^{N-1*} \left[\frac{e^{-i(\epsilon_k - \epsilon_{k'})t} e^{-(\gamma_k + \gamma_{k'})t} - 1}{-i(\lambda_k - \lambda_{k'}^*)} \right] \quad (62)$$

from which it is clear that for $t > 2\pi/|\epsilon_k - \epsilon_{k'}|_{\min}$ the cross terms average to zero, where $|\epsilon_k - \epsilon_{k'}|_{\min}$ is the smallest difference between real parts of the eigenvalues. Then $P_D(t)$ may be approximated by the diagonal term only, i.e.,

$$P_D(t) = \Gamma_{N-1} \sum_k |f_k^{N-1}|^2 \left[\frac{1 - e^{-2\gamma_k t}}{\gamma_k} \right]. \quad (63)$$

This approximation also applies to the molecular-state populations $|a_j(t)|^2$. Since these are a superposition of N terms oscillating at what will in general be incommensurate frequencies, these will not show true Rabi oscillations. Examination of their time behavior will show oscillations on several time scales with a gradual multiexponential decay superimposed. A more useful quantity than instantaneous populations with which to measure the time evolution of molecular-state probabilities is then the time-interval averaged probability

$$\langle |a_j(t)|^2 \rangle_{\Delta t} = \frac{1}{\Delta t} \int_{t-\Delta t/2}^{t+\Delta t/2} |a_j(t')|^2 dt', \quad (64)$$

where Δt is the period of slowest oscillation, $\Delta t = 2\pi/|\epsilon_k - \epsilon_{k'}|_{\min}$.

A further alternative to Eq. (56) is to consider the eigenfunctions of \underline{N} as forming a set of independently decaying levels, whence

$$P_D(t) = 2 \int_0^t \sum_k \gamma_k |\psi_k(t')|^2 dt' \quad (65)$$

$$= 2 \int_0^t \sum_k \gamma_k |T_{0k}|^2 e^{-2\gamma_k t'} dt' \quad (66)$$

$$= \sum_k |T_{0k}|^2 (1 - e^{-2\gamma_k t}). \quad (67)$$

In the next section we present results for the dissociative Morse oscillator, using the above expressions to com-

pare the general RFT to the tridiagonal RFT, within the time-independent approximation given by Eq. (19).

$$\lambda_k = \epsilon_k - i\gamma_k, \quad (59)$$

where ϵ_k and γ_k satisfy the sum rules

$$\sum_{j=0}^{N-1} E_j = \sum_{k=0}^{N-1} \epsilon_k, \quad (60a)$$

$$\Gamma_{N-1} = \sum_{k=0}^{N-1} \gamma_k. \quad (60b)$$

Denoting $T_{jk}T_{0k}$ by f_k^j , we rewrite Eq. (58) as the sum of diagonal terms and cross terms:

pare the general RFT to the tridiagonal RFT, within the time-independent approximation given by Eq. (19).

V. RESULTS AND DISCUSSION: MULTIPHOTON EXCITATION AND DISSOCIATION OF A DIATOMIC MOLECULE

Numerical calculations were carried out for the Morse parameters appropriate to the aromatic C-H bond stretch¹⁷ given in Table II. The values for the dissociation energy D and anharmonicity X are identical to those used by Schek *et al.*^{10,18} These yield a ground-state frequency $\omega_e = 3102.4 \text{ cm}^{-1}$ and give a value for C of 26.88. Since only two parameters are necessary to specify a Morse potential, the discrepancies between these values and the corresponding values cited by Schek *et al.*^{10,18} indicate an ambiguity in the molecular parameters of their study,¹⁹ which introduces a small but minor amount of uncertainty into the comparison between the RFA and exact (i.e., third-order Magnus expansion) results. The molecular eigenfunctions were obtained by an eigenfunction expansion in a basis of sine functions defined on a finite interaction region $(0, L)$, $\{\sin[(n + \frac{1}{2})\pi r/L], n=0, 1, 2, \dots, M-1\}$. The equilibrium distance r_0 and the interaction cutoff distance L are also given in Table II. With a basis size of $M=120$ this gave 26 of the 27 bound eigenvalues, of which the first 23 were accurate to seven significant figures, the inaccuracy then increasing to 16% for the

TABLE II. Molecular parameters used to specify the C-H bond stretch.

D	$= 41705.6 \text{ cm}^{-1}$
x	$= 57.7 \text{ cm}^{-1}$
m	$= 0.92987 \text{ amu}$
r_0	$= 1.75a_0$
L	$= 9.0a_0$

26th state. This eigenfunction expansion was used rather than the exact Morse eigenfunctions for simplicity of computation, this basis having previously been used in an R -matrix calculation for multiphoton dissociation of diatomics.¹² It is recognized that a basis of displaced harmonic oscillator functions would give an improved representation of the eigenfunctions, but the level of agreement with the exact results achieved by use of the sine basis was good enough not to warrant the necessary changes.

The dipole matrix elements μ_{ij} were evaluated by numerical quadrature on $(0, L)$ with 192 points. As repeated comparison with the exact time-dependent calculations of Schek *et al.*¹⁰ will be made in this section, the various models they employ will be briefly summarized here. Their effective Hamiltonian H^{eff} refers to a calculation neglecting antiresonant terms [$\underline{M}'(t)$] and including only coupling between adjacent molecular states. They solved this "standard RWA" by diagonalization of the time-independent interaction matrix. This is the tridiagonal RWA and was done in their work for a linear dipole function only. Their I_1 model also employs a linear dipole function and coupling between adjacent molecular states only, but includes all time-dependent terms, i.e., $\underline{M}^D(t)$ and $\underline{M}'(t)$. Their I_2 , I_3^a , and I_3^b models also include all time-dependent terms and now utilize the full dipole matrix μ . These last three models differ only in the form of the dipole function. The linear dipole function was used for I_2 while I_3^a and I_3^b used the exponential dipole function

(Sec. IV) with r^*/r_0 equal to 1.2 and 0.6, respectively. Figure 2 shows the dipole matrix elements μ_{ij} , $j=i+1, i+2, i+3$, as a function of vibrational state i for (a) the linear and (b) the exponential ($r^*/r_0=1.2$) dipole functions. These correspond well to the values used by Schek *et al.*^{10,20}

Our definition of the laser intensity in terms of the Rabi frequency, Eq. (54), is consistent with that of Schek *et al.*¹⁰ although it was not explicitly defined by them. This is evidenced by the results for the truncated Morse oscillator with $N=4$ where the molecular system is nearly harmonic and the tridiagonal RWA gives virtually the same results as the exact time-dependent calculations. For such a system the general RFA will reduce to the tridiagonal RWA for frequencies near resonance with ω_{10} . Figure 3(a) shows our spectra of $P_D(t)$ versus the energy mismatch from ω_{10}

$$\begin{aligned}\Delta &= (\omega_0 - X) - \omega \\ &= (\omega_e - 2X) - \omega\end{aligned}\quad (68)$$

for the $N=4$ system with the linear dipole function, at a field strength of $\omega_R = 10 \text{ cm}^{-1}$. In this frequency range, the results obtained with the general RFA and the tridiagonal RWA are identical. The spectrum obtained by Schek *et al.*¹⁰ for this system using H^{eff} is reproduced for comparison in Fig. 3(b) (Ref. 21) and shows excellent agreement with our results. The I_1 and I_2 results are visually practically identical to H^{eff} (Fig. 3 of Ref. 10) and so have

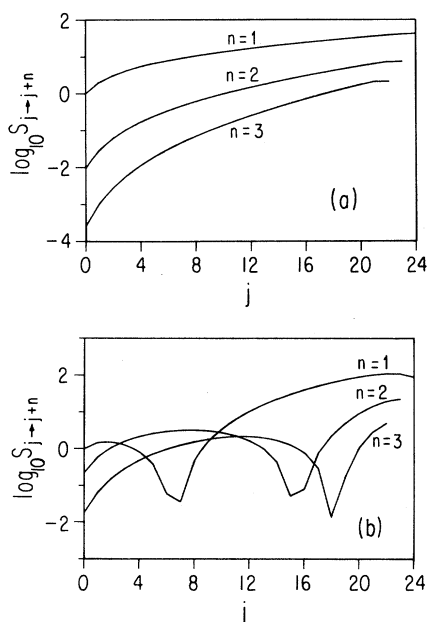


FIG. 2. Radiative coupling matrix elements

$$S_{jj'} = \left| \frac{\langle j | \mu(r) | j' \rangle}{\langle 0 | \mu(r) | 1 \rangle} \right|^2$$

for a Morse oscillator with parameters $D=41705.6 \text{ cm}^{-1}$ and $X=57.7 \text{ cm}^{-1}$ ($\omega_e=3102.4 \text{ cm}^{-1}$). The dipole function is (a) $\mu(r)=kr$ and (b) $\mu(r)=kre^{-r/r^*}$, $r^*=1.2r_0$ where r_0 is the equilibrium distance (Table II). Matrix elements are shown for $j'=j+n$, $n=1, 2, 3$.

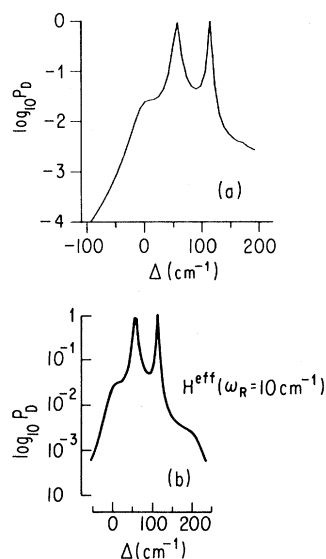


FIG. 3. (a) Frequency dependence of the dissociation probability $P_D(t)$ of a truncated Morse oscillator ($N=4$). The laser frequency is expressed in terms of Δ where $\Delta = \omega_e - 2X - \omega$ [Eq. (68)]. The parameters of the Morse oscillator are given in Table II. The linear dipole function was used, $\mu(r)=kr$. The decay width $\Gamma_{N-j}=X/20$. The pulse duration $t=200 \text{ cm}$ (6.67 ns) and the laser intensity $\omega_R = 10 \text{ cm}^{-1}$. The spectrum shown was obtained with the RFA; the results of the tridiagonal RWA were identical to these. (b) Frequency dependence of $P_D(t)$ for this system, obtained by Schek *et al.* (Ref. 10) using H^{eff} (Ref. 21). Reproduced from Fig. 3 of Ref. 10.

not been reproduced here. Physically, the excellent agreement here between all four models, i.e., the RFA, the tridiagonal RWA (H^{eff}), I_1 and I_2 , is due to three reasons. At low laser intensity the antiresonant terms [$P'(t)$] are relatively unimportant so the tridiagonal RWA gives the same results as I_1 . Secondly, the truncated system is nearly harmonic so that the RFA reduces to the tridiagonal RWA. Finally, the matrix elements μ_{ij} decrease by several orders of magnitude going progressively away from the diagonal (Fig. 2), as expected for a linear dipole function integrated between near harmonic functions. Thus I_2 will give essentially the same results as I_1 . The close equivalence of all four different models for this truncated system confirms the consistency of definition (54) as the Rabi frequency ω_R , throughout all the calculations, both those of Schek *et al.* and ours. We now discuss our results.

Figures 4 and 5 show spectra of $P_D(t)$ vs Δ for the entire bound level system, $N=27$, at two values of field strength, $\omega_R=350\text{ cm}^{-1}$ and $\omega_R=577\text{ cm}^{-1}$, respectively. The pulse duration is $t=200\text{ cm}$ (6.67 ns). In each figure the results of both the general RFA [Eq. (19)] and the tridiagonal RWA are shown for the linear dipole function. There is now a dramatic difference between the effectiveness of the general RFA and the tridiagonal RWA in describing excitation up to the highest levels of the vibrational manifold. At the lower intensity, $\omega_R=350$ (Fig. 4), the tridiagonal RWA shows dissociation greater than 10^{-8} only for a very narrow range of frequencies near $\Delta=1200\text{ cm}^{-1}$ ($\omega\sim\omega_{10}/2$), where a series of equally spaced-multiphoton resonances are apparent on finer resolution [Fig. 4(b)]. The RFA, however [Fig. 4(a)], not only

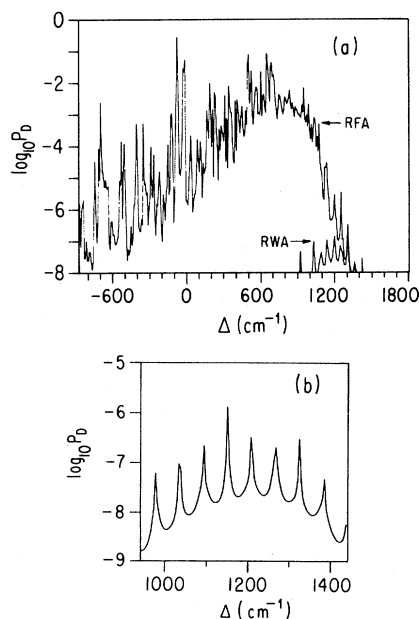


FIG. 4. Spectra of $P_D(t)$ as a function of Δ for the entire bound-level system of the Morse oscillator of Table II ($N=27$) with the linear dipole function. $\Gamma_{N-1}=X/20$; $t=200\text{ cm}$ (6.67 ns); $\omega_R=350\text{ cm}^{-1}$. In (a) the results from both the RFA and the tridiagonal RWA are shown; (b) is a finer resolution plot of the tridiagonal RWA spectrum.

gives significant dissociation over the entire frequency range, $\Delta=1200\text{ cm}^{-1}$ to $\Delta=-200\text{ cm}^{-1}$ ($\omega\sim\omega_{10}/2$ to $\omega\sim\omega_{10}$), but also shows good agreement with the spectra obtained from the full-time dependent calculation for model I_2 , reproduced for comparison in Fig. 6. The qualitative form of the spectrum is well reproduced, showing a broad maximum at a positive value of Δ ($\omega<\omega_{10}$) which corresponds to a frequency considerably greater than the value predicted for a 26 photon $j=0\rightarrow 26$ resonance.¹⁰ Quantitatively, our dissociation probability is a factor of 10^1-10^3 too low at higher frequencies, but the leading edge of the spectrum on the low-frequency side is well reproduced. The relatively minor differences from the exact results which may amount to up to 3 orders of magnitude in $P_D(t)$ may be partially due to the difference in basis functions (affecting μ_{ij}) and eigenvalues, to both of which the general RFT is sensitive, but is probably primarily due to neglect of the time-dependent terms $\underline{P}(t)$ and $\underline{P}'(t)$.

The replacement of the regular resonance structure of the tridiagonal RWA results by the highly irregular dense resonance structure of the RFA results reflects the rich and irregular structure seen in the exact time-dependent results.¹⁰ Series of equally spaced resonances are to be expected within a global RWA when only radiative coupling between adjacent states is included; the equal spacing is a result of the quadratic anharmonicity of Morse eigenvalues.¹⁰ It is the availability of additional absorption pathways involving radiative coupling between nonadjacent states which gives rise to the additional resonance peaks both in the RFA and exact calculations. For a 27 level anharmonic system this effect is particularly dramatic and is of course a corollary of the increased dissociation probability relative to the tridiagonal RWA.

Similar behavior is seen at the higher intensity, $\omega_R=577\text{ cm}^{-1}$, in Fig. 5. This is to be compared with

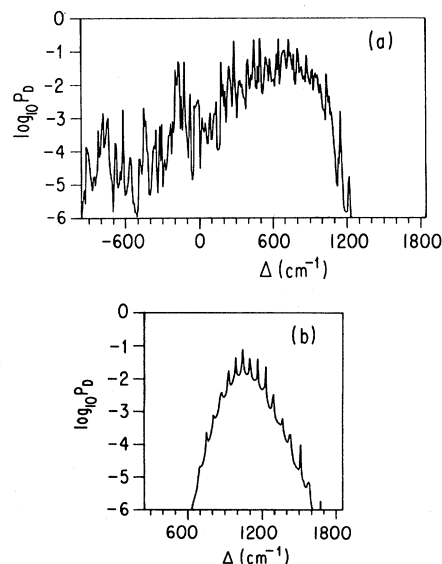


FIG. 5. Spectra of $P_D(t)$ as a function of Δ for the model of Fig. 4 at a laser intensity $\omega_R=577\text{ cm}^{-1}$: (a) shows the RFA result and (b) the tridiagonal RWA result.

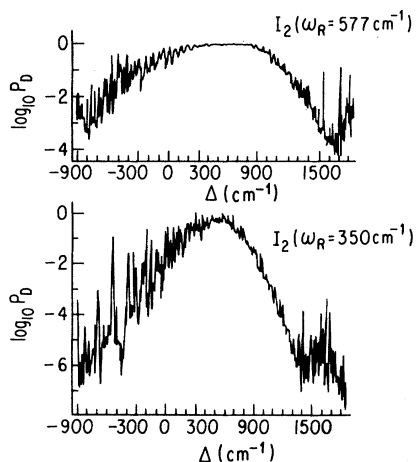


FIG. 6. Spectra of $P_D(t)$ as a function of Δ for the Morse oscillator of Ref. 10 ($N=27$) obtained by Schek *et al.* (Refs. 10 and 21) using model I_2 (linear dipole function, full dipole coupling matrix, and third-order Magnus expansion). (a) $\omega_R=350$ cm^{-1} . (b) $\omega_R=577$ cm^{-1} . Pulse duration $t=200$ cm (6.67 ns). Reproduced from Figs. 10 and 11 of Ref. 10.

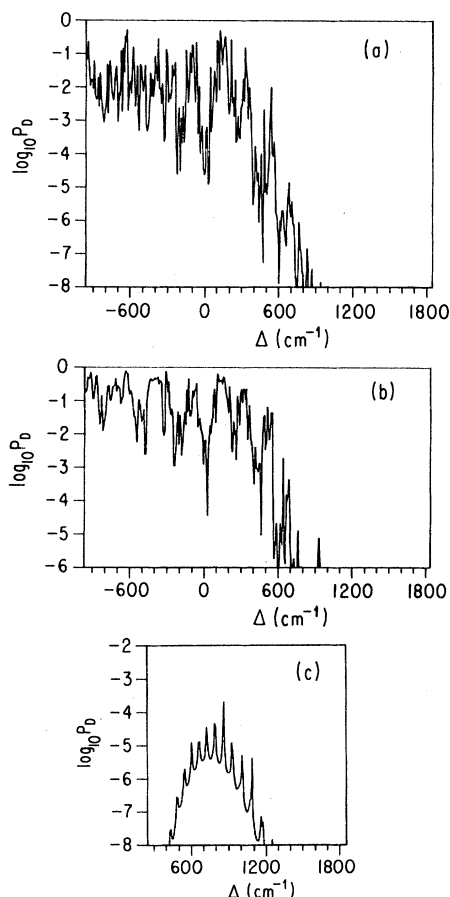


FIG. 7. Spectra of $P_D(t)$ as a function of Δ for the model of Fig. 4 with the exponential dipole function, $\mu(r) = kr \exp(-r/r^*)$, $r^* = 1.2r_0$. (a) The RFA spectrum at a laser intensity $\omega_R=350$ cm^{-1} . The maximum value of $\log P_D(t)$ from the tridiagonal RWA at this intensity is -11 . (b) The RFA spectrum at a laser intensity $\omega_R=577$ cm^{-1} . (c) The tridiagonal RWA spectrum at $\omega_R=577$ cm^{-1} .

Fig. 6(b). For the tridiagonal RWA the greater intensity now causes the off-resonance energies to be dominated by the greater couplings, allowing several orders of magnitude more dissociation as a result of intensity saturation. The intensity dependence of $P_D(t)$ will be discussed in detail below.

Results for the exponential dipole function with $r^*/r_0=1.2$ are shown in Fig. 7, for $\omega_R=350$ and 577 cm^{-1} . Comparison with the exact results for model I_3^a (Fig. 8) is again very close for the general RFA and extremely poor for the tridiagonal RWA.

A comparison of the results given by the two dipole functions shows several features deriving from the very different variation in dipole elements (Fig. 2). Firstly, comparing the tridiagonal RWA results at $\omega_R=577$ cm^{-1} [Figs. 5(b), 7(c)] it is evident that the exponential dipole function gives about 3 orders of magnitude less dissociation at its maximum, and that dissociation occurs over a smaller range of frequencies, with the maximum displaced to lower Δ (i.e., higher frequency ω). In both cases the maximum is at a value of Δ well above the value $\Delta=0$ which corresponds to $\omega=\omega_{10}$. The smaller dissociation probability for the exponential model reflects the sharp drop in the radiative coupling elements $\mu_{i,i+1}$ for $i=4-8$, which leads to an impasse in absorption. For a Morse oscillator k -photon resonance coupling between molecular levels $i-k$ and i occurs at $\Delta=(2i-k-1)X$.^{19,21} Thus the maximum at $\Delta=19X$ for the linear model can be attributed to the overlap of a large number of resonances, both low order ones between intermediate states, e.g., $i=11$, $k=2$, and high-order resonances terminating in higher vibrational states, e.g., $i=14$, $k=8$. By comparison, the radiative bottleneck of the exponential model reduces contributions from the latter type of resonance as well as generally impeding the population of higher levels. Thus in

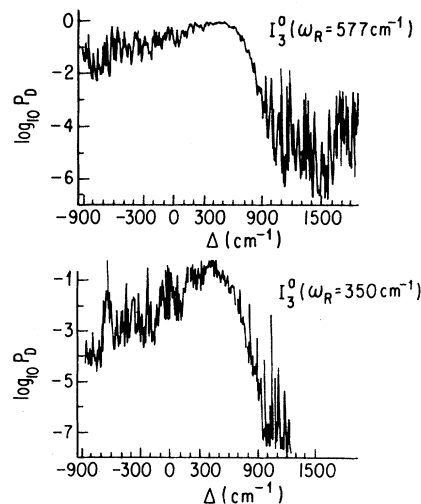


FIG. 8. Spectra of $P_D(t)$ as a function of Δ for the Morse oscillator of Ref. 10 obtained by Schek *et al.* (Refs. 10 and 21) using model I_3^a (exponential dipole function, $r^*=1.2r_0$, full dipole coupling matrix, third-order Magnus expansion). (a) $\omega_R=350$ cm^{-1} . (b) $\omega_R=577$ cm^{-1} . Pulse duration $t=200$ cm (6.67 ns). Reproduced from Figs. 10 and 11 of Ref. 10.

addition to having a uniformly lower dissociation probability than the linear model, there is a drastic reduction at large values of Δ and the position of maximum dissociation shifts downward to $\Delta=16X$.

This displacement to lower values of Δ is also seen in the RFA results (Figs. 4, 5, and 7) and in the exact results of Schek *et al.* (Figs. 6 and 8). The large amount of dissociation now seen for $\Delta < 0$ ($\omega > \omega_{10}$) is due to the presence of radiative coupling between nonadjacent molecular states, allowing direct $i \rightarrow i+j$, $j > 1$ transitions and enhancing k -photon resonances between the ground state $i=0$ and $i=m$, where $m \neq k$. High values of P_D persist to much larger negative Δ for the exponential function, presumably because the $\mu_{i,i+2}$ and $\mu_{i,i+3}$ matrix elements are much larger relative to $\mu_{i,i+1}$ for the exponential model (Fig. 2).

A detailed analysis of the structure of the RFA spectra is complicated by the large number of resonances involved and by the frequency dependence of the matrix \underline{N} involved, i.e., of the couplings included. The sharp irregular structure represents a dense overlap of resonances, and is not due to numerical artifact. The exact results show similar dense structure (Figs. 6 and 8) but comparison of individual peaks is not warranted due to the possible slight differences in molecular parameters.¹⁹ One prominent feature of the RFA results not shown by the exact results is the peak between $\Delta = -100$ and -50 cm^{-1} for the linear dipole model [Figs. 4(a) and 5(a)]. This can be tentatively assigned to a superposition of a six-photon resonance between states $i=0$ and 7, and an eight-photon resonance between states $i=0$ and 10. Adding a shift to q_7 and q_{10} in turn effectively causes these transitions to become off resonant without affecting other states. This changes the spectrum in the vicinity of $\Delta=100$, shifting and decreasing the peak with little effect elsewhere, which is positive evidence for such an assignment. Addition of the time-dependent matrices $\underline{P}(t)$ and $\underline{P}'(t)$ would be expected to reduce the restrictive resonance requirements somewhat, perhaps submerging the peak in a uniform background in the exact calculations (Fig. 6). However, more important than the complex resonance structure, which would be washed out by a finite bandwidth calculation, is the extent to which the envelope of dissociation probabilities approximates that of the exact results.

The only major feature of the $N=27$ spectrum which is not given by the RFA is the small secondary peak at very low frequencies, near $\Delta=1600 \text{ cm}^{-1}$ (Fig. 6). In the range $\Delta=1600$ to 1900 cm^{-1} the general RFA and the tridiagonal RWA gave identical results. At these frequencies, $\omega < \omega_{10}/2$, multiphoton absorption is required to reach even the first excited state. From the discussion of the relation between the time-independent interaction matrix \underline{N} and the fully quantized radiation-matter interaction Hamiltonian (Sec. IV), it is clear that \underline{N} contains no couplings describing simultaneous absorption of several photons in a single molecular transition, so it is to be expected that the time-independent approximation of Eq. (19) will not be able to describe such excitations. [Since such processes will be described in the fully quantized formalism by sequential processes involving non-energy-conserving steps, it will be necessary to include the antiresonant ma-

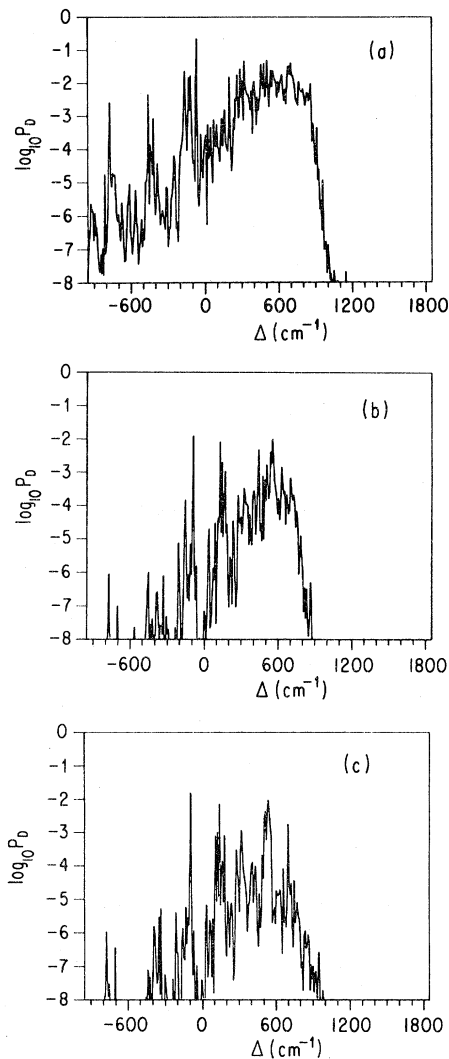


FIG. 9. Spectra of $P_D(t)$ as a function of Δ for the model of Fig. 4 using the linear dipole function with twice the dipole coupling element strength in selected blocks of the matrix μ . The laser intensity $\omega_R = 175 \text{ cm}^{-1}$. The elements μ_{ij} have an extra factor of 2 for (a) $i, j \leq 9$, (b) $9 < i, j < 19$, and (c) $i, m \geq 19$.

trix $\underline{P}'(t)$ for a full description in the semiclassical representation.] Apart from this feature, however, it appears that the general RFT is managing to include essentially all the important couplings and off-resonance energies relevant to the overall multiphoton process in the time-independent matrix \underline{N} .

Of particular relevance to the use of the general RFT for polyatomic systems is the result of uniformly varying the strength of the dipole couplings in different regions of the molecular-level structure, shown in Fig. 9 for the linear dipole model. For a given field strength, $\omega_R = 175 \text{ cm}^{-1}$, the matrix elements μ_{ij} were multiplied by a factor of 2 in three different blocks of \underline{N} : (i) $i, j \leq 9$, (ii) $9 < i, j < 19$, and (iii) $i, j \geq 19$. This is equivalent to using the true couplings in each of these regions with an effective-field strength of $\omega_R = 350 \text{ cm}^{-1}$ in the appropriate block. The dissociation probability obtained from the

general RFA for each of these artificial systems is given in Figs. 9(a)–9(c), respectively. The factor of 2 increase in coupling in the lowest block, (i) $i, j \leq 9$ [Fig. 9(a)], increases the dissociation probability $P_D(t)$ for the general RFA from that at $\omega_R = 175 \text{ cm}^{-1}$ to that seen at twice the field strength, $\omega_R = 350 \text{ cm}^{-1}$ [Fig. 4(a)]. However, $P_D(t)$ is relatively insensitive to the effective-field strength in the other two blocks, (ii) and (iii). A similar effect for the tridiagonal RWA is achieved by inserting a factor of 2 in the block, (ii) $9 < i, j < 19$, while the other two regions have little effect here. Thus the general RFA is very sensitive to the couplings in the lowest, nearly harmonic part of the molecular-level structure, which is that which will be best characterized for polyatomic species, whereas the tridiagonal RWA is more sensitive to the region where anharmonicity effects become important. (In either case, however, the RFA is orders of magnitude better than the RWA.)

The calculation of these spectra using the RFA is a very quick and easy process, requiring only the selection of the nonzero off-diagonal elements at each frequency, followed by diagonalization of \underline{N} and subsequent summation to evaluate $P_D(t)$, using Eq. (63). This diagonal approximation, Eq. (63), is computationally the simplest and most stable expression for the dissociation probability. A 350 point (frequency) spectrum for $N=27$ took typically 40 mins CPU (central processing unit) time on a Digital Equipment Corporation VAX-11/780 computer. The use of the diagonal approximation, Eq. (63), does require some justification. Since the general RFT is defined to minimize $|q_j|$, it might be thought that it would be possible to have a near degeneracy in ϵ_k , the real part of the eigenvalues of \underline{N} , which would give rise to very large values of the maximum period $\Delta t = 2\pi / |\epsilon_k - \epsilon_{k'}|_{\min}$ and persistence of nonzero contributions from the cross terms in Eq. (62). However, any degeneracies in q_j will always be split by the off-diagonal couplings. In first-order perturbation theory, for an isolated pair of levels i and j , the splitting would be equal to $2D_{ij}$. Thus the noncrossing of the dressed molecule-field states will always ensure a maximum oscillatory period, which is usually on the order of 10^{-12} sec in this system. Comparison of $P_D(t)$ evaluated using Eq. (63) with the exact expression, Eq. (58), confirmed the validity of the diagonal approximation for all frequencies and time scales studied in this work.

Figure 10 shows the time dependence of $P_D(t)$ for a frequency ω near the maximum of Fig. 4(a) ($\Delta = 532 \text{ cm}^{-1}$)

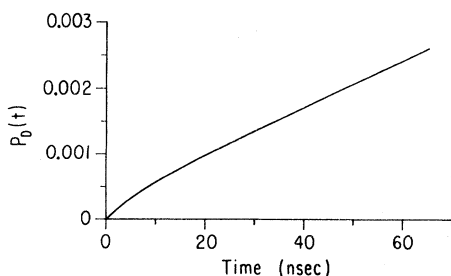


FIG. 10. Time dependence of the dissociation probability $P_D(t)$ for the model of Fig. 4 at $\Delta = 532 \text{ cm}^{-1}$, and $\omega_R = 350 \text{ cm}^{-1}$.

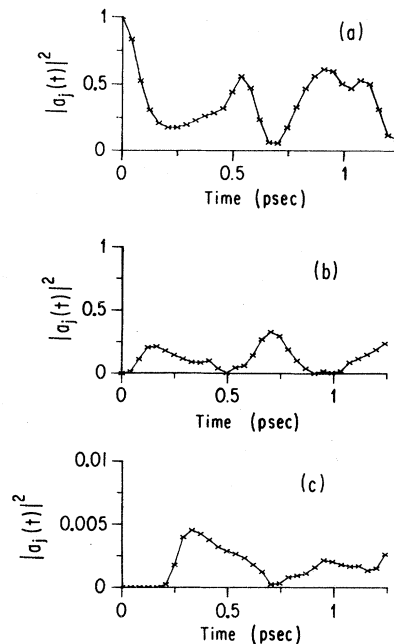


FIG. 11. Time evolution of the instantaneous level populations $|a_j(t)|^2$ for the model of Fig. 4 at $\Delta = 532 \text{ cm}^{-1}$ and $\omega_R = 350 \text{ cm}^{-1}$. In (a) $j=0$, in (b) $j=2$, and in (c) $j=14$.

at the field strength $\omega_R = 350 \text{ cm}^{-1}$. This displays the monotonic increase toward unity predicted by Eqs. (55) and (56) for a system in which the coupling is strong enough that all the independent dressed states $|\psi_k\rangle$ have nonzero decay widths induced by effective coupling of all molecular states to the single predissociative molecular state ϕ_{N-1} .

The time evolution of the molecular-state populations is summarized in Figs. 11 and 12 for the same frequency and intensity. The instantaneous molecular populations $|a_j(t)|^2$ are plotted on a time scale of picoseconds for $j=0 \rightarrow 2$ and $0 \rightarrow 14$ in Fig. 11. Calculations on smaller time scales show no additional oscillatory structure, so this is the smallest time scale in the coupled molecule-field system. Figures 11(b) and 11(c) show the increasing delay time for populating successively higher molecular states. Irregular oscillatory behavior sets in after this delay time. It is interesting that the delay time for $j=14$ (which is in

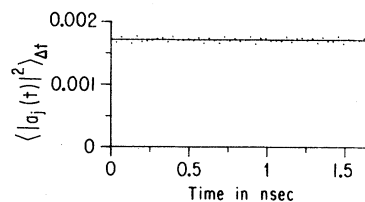


FIG. 12. Time-averaged level population $\langle |a_j(t)|^2 \rangle_{\Delta t}$ as a function of time for the model of Fig. 4 at $\Delta = 532 \text{ cm}^{-1}$ and $\omega_R = 350 \text{ cm}^{-1}$. The dotted line (.....) shows $\langle |a_j(t)|^2 \rangle_{\Delta t}$ for $j=14$ with $\Delta t = 8.27 \text{ ps}$. The solid line (—) is the diagonal approximation to the instantaneous level population $|a_j(t)|^2$ [from Eq. (55)] for $j=14$.

the middle of the molecular-level range) approximately equals the time after which the initial monotonic decrease in the ground state, $j=0$, is succeeded by oscillatory behavior. This indicates a departure from the two-level type behavior seen for resonantly excited N -level systems,⁹ in which the population effectively oscillates alternately between the lowest level $j=0$ and the highest level $j=N-1$. Figure 12 shows on a larger time scale (nanoseconds) the diagonal approximation to the instantaneous molecular population given in Eq. (55) and the time-interval averaged populations $\langle |a_j(t)|^2 \rangle_{\Delta t}$ [Eq. (64)] for $j=14$. The average was performed over a time interval $\Delta t=8.27$ psec. Apart from small fluctuations, the time-averaged result is equivalent to the diagonal approximation, which shows virtually no decay on this time scale. The diagonal approximation (as, also, for this value of Δt , the time-averaged result) is incorrect at $t=0$ where the cross terms are needed to cancel out the diagonal contribution to Eq. (55) in order to obtain the initial condition $|a_j(0)|^2 = \delta_{j0}$ at $t=0$.

The intensity dependence of $P_D(t)$ was calculated for both forms of the dipole function and is shown in Fig. 13. Several interesting points are raised here. The superiority of the RFA in describing excitation in the lower intensity

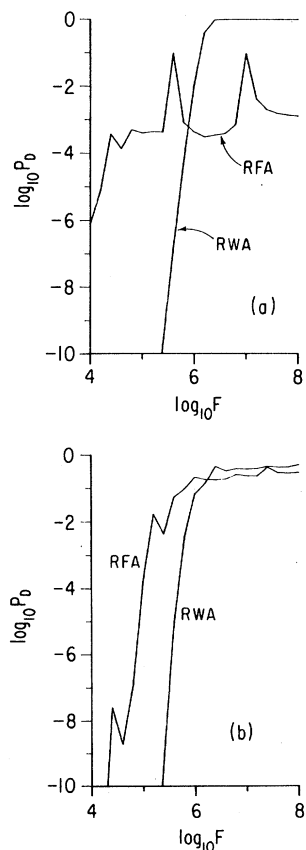


FIG. 13. Intensity dependence of $P_D(t)$ for the model of Fig. 4 with both the linear and exponential dipole functions at $\Delta=532$ cm^{-1} . The intensity is measured as $F=\omega_R^2$ in cm^{-2} . (a) shows the results given by the RFA and by the tridiagonal RWA for the linear dipole function; (b) shows the corresponding results for the exponential dipole function.

range persists in both examples up to $\omega_R^2 \sim 10^6$ cm^{-2} , but at very (unphysically) high intensities the tridiagonal RWA may give higher saturation dissociation probabilities than the general RFA. Secondly, both time-independent approximations produce saturation, but the increase in $P_D(t)$ with intensity is not monotonic. This is also seen in the exact calculations.¹⁰ However, whereas the exact time-dependent calculations always reach saturation at $P_D(t)$ equal to unity, the tridiagonal RWA and the general RFA results do not necessarily saturate at unity for very high intensities. At such extreme intensities the global RWA fails and the contribution of both antiresonant and proresonant matrices, $\underline{P}'(t)$ and $\underline{P}(t)$, is significant. We briefly consider this now. The question of intensity dependence is simplest for the tridiagonal RWA, for which $\underline{P}(t)=0$. It is clear from the work of Schek *et al.*¹⁰ that at intensities of $\omega_R > 350$ cm^{-1} , $\underline{P}'(t)$ gives a significant contribution for the tridiagonal case since the spectra of I_1 and H^{eff} differ by several orders of magnitude. Over the intensity range $\omega_R^2 = 10^5 - 10^6$ cm^{-2} at $\Delta = 532$ cm^{-1} the dissociation probability given by H^{eff} is 4 orders of magnitude too low. At lower intensities a perturbative analysis of the matrix \underline{N} , identifying further $N \times N$ diagonal blocks of the infinite Floquet matrix of the form $\underline{N} + 2k\omega \underline{1}$, $k=1, 2, \dots$, which are coupled to \underline{N} by one-photon radiative couplings, would be possible. However, the extremely high intensities used in the exact calculations, combined with the increase of both radiative couplings and anharmonicity for higher vibrational states, render perturbation theory invalid, at least in the upper levels. Even expansion of \underline{N} to a $3N \times 3N$ supermatrix with diagonal blocks $\underline{N} + 2\omega \underline{1}$, \underline{N} , $\underline{N} - 2\omega \underline{1}$, and associated off-diagonal coupling blocks, followed by exact diagonalization and projection onto the initial and final molecular states to evaluate $a_{N-1}(t)$ which is then used in Eq. (58) as before, did not account for all the increase in dissociation probability between H^{eff} and I_1 at $\omega_R = 350$ cm^{-1} . Inclusion of more blocks $\underline{N} + 2k\omega \underline{1}$ is impractical. Since $\underline{P}(t) \neq 0$ for the RFA and furthermore contains slower oscillating terms than $\underline{P}'(t)$, the relative role of these terms as a function of intensity is an additional question for the RFA. In the absence of exact time-dependent calculations at lower intensities, it is not possible at this stage to say when either $\underline{P}(t)$ or $\underline{P}'(t)$ become important corrections to the RFA, although there is clearly some contribution at $\omega_R = 350$ cm^{-1} . Note that these intensities are too high to be of physical relevance—for the linear dipole function, $\omega_R = 350$ cm^{-1} corresponds to an intensity $I = 10^{15}$ W/cm^2 . However, the general RFA is applicable to, and we hope will be most useful for larger molecular systems, for which considerably lower field strengths are sufficient to give excitation to upper levels. Perturbation theory would then be sufficient to correct the RFA results.

Although not physically relevant and thus not affecting the use of the general RFA, the high-intensity behavior of Fig. 13 does illustrate the interplay between the two basic factors influencing excitation to higher levels: minimizing the diagonal elements of \underline{N} (off-resonance energies) and maximizing the off-diagonal elements of \underline{N} (molecular-level couplings and laser field strength). These together determine the efficacy of a given \underline{N} in describing transfer-

ence of population from the lowest to the highest level and thereby dissociation (assuming Γ_{N-1} fixed). At extremely high intensities the off-diagonal terms dominate. These observations relate to the more fundamental question of whether the general RFA is providing us with the optimal time-independent matrix \underline{N} with which to approximate absorption from some initial state (in this case the ground state) to some final state (in this case the highest bound state) at any given frequency ω . At absurdly high saturation intensities, when the off-diagonal elements are orders of magnitude larger than the diagonal elements, it clearly does not. However, at the lower intensities (and those relevant to multiphoton processes in small polyatomic molecules will be much smaller than the intensities used in this work for a model diatomic molecule) the RFA appears to be providing a frequency-dependent matrix \underline{N} which contains most of the information pertaining to the dynamics. The importance of this flexibility, namely the frequency dependence of the matrix structure, is seen when the off-diagonal elements appropriate to a particular frequency ω_1 are combined with the diagonal elements appropriate to a second frequency ω_2 , close to ω_1 . The resulting $P_D(t)$ at ω_2 is less when evaluated with the off-diagonal couplings appropriate to ω_1 than when evaluated with its correct couplings. This change can be as much as a factor of 10^2 for two frequencies differing by 10 cm^{-1} . However, the general question, whether our choice of \underline{q} in this general RFA, Eq. (26), produces the optimum time-independent matrix \underline{N} at a particular frequency and intensity is not an easy one. Some indication would be provided by a time-dependent calculation in the global RWA, i.e., neglecting only the antiresonant matrix $\underline{M}'(t)$, and retaining the full dipole array μ . At present the discrepancy of a factor of 10^1 – 10^3 between the full-time dependent calculation and our general RFA could be due to the contribution of relevant terms in either of the two transformed time-dependent matrices $\underline{P}(t)$ [from $\underline{M}(t)$] and $\underline{P}'(t)$ [from $\underline{M}'(t)$], or to apparently minor differences in the physical models. Since any useful RFA will be used in the context of the global RWA, which will be of greater validity for the considerably reduced intensities used for excitation of polyatomic molecules, any comparative studies should be made with reference to the time-dependent calculation employing only the full matrix $\underline{M}(t)$, i.e., the global RWA.

Although as discussed in Sec. II it will not in general be possible to define \underline{q} so as to include all couplings from $\underline{M}(t)$ in \underline{N} , the possible existence of a well-defined maximum number of off-diagonal elements for which N values of q_j will eliminate the time dependence is worth further study. Since the matrix \underline{N} is diagonalized, the sizes of the off-diagonal elements relative to the diagonal elements are also relevant to the optimization of \underline{N} . This was seen in the intensity dependence studies. One is really asking how the eigenvalues (in particular $\{\gamma_k\}$) of a symmetric complex matrix are affected by (i) the distribution and size of the off-diagonal elements and (ii) the size of the diagonal elements. The variation in eigenvectors is also relevant [Eq. (55)]; for nondissociative systems ($\Gamma_{N-1}=0$) this is the only relevant question. For $N > 3$ this is a problem which may not be soluble exactly.

A final comment on the particular choice of q_j defined in the general RFT, Eq. (26), is that it does allow an interpretation in terms of the fully quantized radiation-matter formalism which would be lost if q_j were not defined in terms of the molecular frequencies ω_{ij} and the laser frequency ω , alone. Furthermore, in the fully quantized formalism there is a strong physical rationale for the effectiveness of this choice of \underline{q} . The molecule-field states included are those most nearly resonant with the initial state. In perturbation theory these would be making the greatest contribution to the dressed states into which the initial state is transformed by the interaction—provided all couplings are equal. The relative sizes of the couplings is a secondary factor at all but the most extreme intensities.

VI. SUMMARY AND CONCLUSIONS

By introducing a new and general rotating-frame transformation (the general RFT), the time-dependent Schrödinger equation for a multilevel system in the presence of a coherent oscillatory field has been put into a representation in which most of the molecular couplings and energy defects pertinent to the multiphoton dynamics are contained in a time-independent interaction matrix. Neglect of all antiresonant time-dependent terms (the global RWA) and of the remaining proresonant time-dependent couplings reduces the problem to the solution of an eigenvalue equation, referred to as the general rotating-frame approximation (the general RFA). The flexibility of the RFT, resulting in a *frequency-dependent* time-independent interaction matrix \underline{N} , renders it an extremely powerful and general technique for following the coherent multiphoton excitation dynamics of many-level systems. Application of the general RFA to multiphoton absorption and dissociation of a diatomic molecule, modeled as a Morse oscillator, by very intense infrared laser radiation showed close agreement (within a factor of 10^1 – 10^3 —as opposed to 10^{12}) with the results of an exact time-dependent calculation performed using the Magnus expansion to third order.¹⁰ For such an anharmonic system the general RFA proved to be far superior to the tri-diagonal RWA, the time-independent approximation used in previous calculations for coherent multiphoton excitation of multilevel systems, to which the general RFA reduces for harmonic systems. The far greater sensitivity of the dissociation probability to the relative coupling strengths in the lower region of the molecular-level structure than in the upper region suggests that the general RFA will be a very useful tool for quantitative study of the multiphoton excitation of small polyatomics. Furthermore, the notion of resonant pathways of absorption automatically generated by the restriction of minimizing the values $|q_j|$ suggests a natural way of reducing the large number of molecular states in a polyatomic molecule to a small subset which should give the major contribution to multiphoton absorption. We are currently applying the method to the multiphoton excitation and dissociation of ozone by a single infrared laser, for which some experimental evidence is available.²²

At the high intensities appropriate to laser radiation

fields, the time-independent interaction matrix produced by the general RFT, \underline{N} , can be related to the fully quantized radiation matter Hamiltonian. In the fully quantized representation the effect of the transformation is seen to be a selection from the infinite basis of the finite set of molecule-field states closest in energy to the initial state, subject to the restriction of retaining only one molecule-field state per molecular state. The couplings introduced into \underline{N} by the transformation are all allowed one-photon couplings between this finite set of molecule-field states. The frequency dependence of the general RFT gives it the flexibility to adjust the structure of the matrix \underline{N} to include the appropriate pathways of absorption to the set of molecule-field states closest to resonance with the initial state at each frequency.

The theory of the general RFT can be extended to deal with interactions in the presence of several frequencies. In the particular case of N levels with m frequencies close to resonance with m of the $N(N-1)/2$ possible transitions, it becomes equivalent to the treatment of Einwohner, Wong, and Garrison.⁸ Here it is important to note that, similar to the modulation of off-resonance energies by intensity in the single-frequency case, the relative intensities

$$\underline{A}_1(t, t_0) = -\frac{i}{\hbar} \int_{t_0}^t dt_1 \underline{H}(t_1),$$

$$\underline{A}_2(t, t_0) = \frac{1}{2\hbar^2} \int_{t_0}^t dt_2 \int_{t_0}^{t_2} dt_1 [\underline{H}(t_1), \underline{H}(t_2)],$$

$$\underline{A}_3(t, t_0) = \frac{i}{6\hbar^3} \int_{t_0}^t dt_3 \int_{t_0}^{t_3} dt_2 \int_{t_0}^{t_2} dt_1 \{ [\underline{H}(t_1), [\underline{H}(t_2), \underline{H}(t_3)]] + [[\underline{H}(t_1), \underline{H}(t_2)], \underline{H}(t_3)] \}.$$

In the representation $\vec{c}(t)$ produced by the rotating-frame transformation, Eq. (16), the Hamiltonian becomes [Eq. (18)]

$$\frac{1}{\hbar} \underline{H}(t) = \underline{N} + \underline{P}(t) + \underline{P}'(t). \quad (\text{A3})$$

Since t , the pulse length, is considerably greater than the optical period, $\tau = 2\pi/\omega$, we can replace $\underline{U}(t, t_0)$ by $[\underline{U}(\tau)]^m$ where m is the integral divisor of t by τ . Then

$$\vec{c}(t) \simeq [\underline{U}(\tau)]^m \vec{c}(0). \quad (\text{A4})$$

Evaluating the exponents $\underline{A}_n(\tau, 0)$ we find for $n = 1, 2$

$$\underline{A}_1(\tau, 0) = -\frac{i}{\hbar} \tau \underline{N}, \quad (\text{A5})$$

$$\underline{A}_2(\tau, 0) = \frac{1}{2\hbar^2} \int_0^\tau dt_2 \int_0^{t_2} dt_1 [\underline{N} \underline{V}(t_2) + \underline{V}(t_1) \underline{N}],$$

where $\underline{V}(t) = \underline{P}(t) + \underline{P}'(t)$. $\underline{A}_3(\tau, 0)$ contains integrals of commutators $[\underline{N}, \underline{N} \underline{P}(t_i)]$, $[\underline{N}, \underline{P}(t_i) \underline{P}(t_j)]$, etc.

For effective use of the Magnus expansion, fast convergence is required. Although the convergence properties of the expansion itself are poorly defined, it is, however, meaningful to compare the relative sizes of corresponding terms in different representations for a given Hamiltonian. Thus the form of some of the matrix elements of $\underline{A}_n(\tau, 0)$

of the different field frequencies will play a significant role in the accuracy of the resulting time-independent approximation. Again this may require modification of the minimization principle by which the transforming matrix e^{iqt} is constructed, in order to achieve an optimal time-independent approximation (i.e., an optimal RFA).

ACKNOWLEDGMENT

This research was supported by U. S. Department of Energy Grant No. DE-AC02-78ER04908.

APPENDIX: THE MAGNUS EXPANSION IN A ROTATING FRAME

For a system characterized by a time-dependent Hamiltonian $H(t)$, the Magnus formula gives an expansion of the time evolution operator $U(t, t_0)$ which is unitary to all orders of truncation.²³ In matrix notation,

$$\underline{U}(t, t_0) = \exp[\underline{A}_1(t, t_0) + \underline{A}_2(t, t_0) + \underline{A}_3(t, t_0) + \cdots] \quad (\text{A1})$$

with

obtained from the tridiagonal RFT [Eq. (21)] and from the general RFT [Eq. (26)] are compared in Table III. It is clear that the terms from the tridiagonal RFT which contain Δ_{j_0} as a factor, e.g., $\Delta_{j_0} D_{kl} / \omega^2$, will become very large at high j for anharmonic systems (since $-\Delta_{j_0} \gg \omega$ for j large). This will result in increasingly large contributions from the higher-order terms. However, the minimi-

TABLE III. Form of matrix element components of the integrated exponents $\underline{A}_n(\tau, 0)$ for representations resulting from the tridiagonal RFT and from the general RFT. Entries for $\underline{A}_1(\tau, 0)$ and $\underline{A}_2(\tau, 0)$ provide all possible forms of components for these matrices. For $\underline{A}_3(\tau, 0)$ only the components which differ in the two representations are shown. Here τ is the optical period $2\pi/\omega$. These expressions are correct up to factors of 2π (arising from integration over τ), $1/\hbar^n$ and integral divisors resulting from integration of the higher oscillatory terms $e^{\pm im\omega t}$ which are not relevant to this comparison.

	$\underline{A}_1(\tau, 0)$	$\underline{A}_2(\tau, 0)$	$\underline{A}_3(\tau, 0)$
Tridiagonal	Δ_{j_0} / ω	$D_{jk} D_{lm} / \omega^2$	$(\Delta_{j_0})^2 D_{kl} / \omega^3$
RFT	D_{jk} / ω	$\Delta_{j_0} D_{kl} / \omega^2$	$\Delta_{j_0} D_{kl} D_{pq} / \omega^3$
		$\Gamma_{N-1} D_{kl} / \omega^2$	
General	q_j / ω ($ q_j \leq \omega/2$)	$D_{jk} D_{lm} / \omega^2$	
RFT	D_{jk} / ω	$D_{kl} / 2\omega$	$D_{kl} / 4\omega$
		$\Gamma_{N-1} D_{kl} / \omega^2$	$D_{kl} D_{pq} / 2\omega^2$

zation of $|q_j|$ in the general RFT replaces these terms by terms of order D_{kl}/ω in which the effect of the anharmonicity is now only indirectly present, in D_{kl} , as in all other terms. For a given truncation of the expansion at

some order n , the general RFT should converge faster than the tridiagonal RFT for an anharmonic molecular system and will therefore provide a better representation for the Magnus expansion.

- ¹For review articles, see J. Jortner, SPIE **113**, 88 (1977); N. Bloembergen and E. Yablonovitch, Phys. Today **31**, 23 (May 1978); C. D. Cantrell, S. M. Freund, and J. L. Lyman, in *Laser Handbook* (North-Holland, Amsterdam, 1978); P. A. Schulz, Aa. S. Sudbo, D. J. Krajnovich, H. S. Kwok, Y. R. Shen, and Y. T. Lee, Ann. Rev. Phys. Chem. **30**, 379 (1979); R. G. Harrison and S. R. Butcher, Contemp. Phys. **21**, 19 (1980).
- ²N. Bloembergen, Opt. Commun. **15**, 416 (1975); I. Schek and J. Jortner, J. Chem. Phys. **70**, 3016 (1979); B. Carmeli, I. Schek, A. Nitzan, and J. Jortner, *ibid.* **72**, 1928 (1980).
- ³J. L. Lyman, J. Chem. Phys. **67**, 1868 (1977); J. A. Horsley, J. Stone, M. F. Goodman, and D. Dows, Chem. Phys. Lett. **66**, 461 (1979).
- ⁴P. Kolodner, C. Winterfeld, and E. Yablonovitch, Opt. Commun. **20**, 119 (1977); J. G. Black, P. Kolodner, M. J. Schultz, E. Yablonovitch, and N. Bloembergen, Phys. Rev. A **19**, 704 (1979).
- ⁵J. Stone and M. F. Goodman, J. Chem. Phys. **71**, 408 (1979).
- ⁶E. R. Grant, P. A. Schulz, Aa. S. Sudbo, Y. R. Shen, and Y. T. Lee, Phys. Rev. Lett. **40**, 115 (1978); E. Thiele, J. Stone, and M. F. Goodman, Chem. Phys. Lett. **66**, 457 (1979).
- ⁷J. R. Ackerhalt and J. H. Eberly, Phys. Rev. A **14**, 1705 (1976).
- ⁸T. M. Einwagner, J. Wong, and J. C. Garrison, Phys. Rev. A **14**, 1452 (1976).
- ⁹Z. Bialynicka-Birula, I. Bialynicka-Birula, J. H. Eberly, and B. W. Shore, Phys. Rev. A **16**, 2038 (1977); J. H. Eberly, B. W. Shore, Z. Bialynicka-Birula, and I. Bialynicka-Birula, *ibid.* **16**, 2048 (1977); B. W. Shore and J. H. Eberly, Opt. Commun. **24**, 83 (1978); R. J. Cook and B. W. Shore, Phys. Rev. A **20**, 539 (1979); B. W. Shore and R. J. Cook, *ibid.* **20**, 1958 (1979).
- ¹⁰I. Schek, J. Jortner, and M. L. Sage, Chem. Phys. **59**, 11 (1981).
- ¹¹S. Leasure and R. E. Wyatt, Chem. Phys. Lett. **61**, 625 (1979); Opt. Eng. **19**, 46 (1980); J. Chem. Phys. **73**, 4439 (1980); S. Leasure, K. Milfield, and R. E. Wyatt, *ibid.* **74**, 6197 (1981); S. I. Chu, J. V. Tietz, and K. K. Datta, *ibid.* **77**, 2968 (1982).
- ¹²S. I. Chu, J. Chem. Phys. **75**, 2215 (1981); C. Leforestier and R. E. Wyatt, Phys. Rev. A **25**, 1250 (1982); K. B. Whaley and J. C. Light, J. Chem. Phys. **77**, 1818 (1982).
- ¹³J. H. Shirley, Phys. Rev. B **138**, 979 (1965).
- ¹⁴R. Loudon, *The Quantum Theory of Light* (Clarendon, Oxford, 1973).
- ¹⁵F. R. Gantmacher, *Matrix Theory* (Chelsea, New York, 1960), Vol. II.
- ¹⁶F. H. M. Faisal and J. V. Moloney, J. Phys. B **14**, 3603 (1981).
- ¹⁷R. L. Swofford, M. E. Long, and A. C. Albrecht, J. Chem. Phys. **65**, 179 (1976).
- ¹⁸I. Schek, M. L. Sage, and J. Jortner, Chem. Phys. Lett. **63**, 230 (1979).
- ¹⁹A related earlier study by I. Schek and J. Jortner of multiphoton resonances in excitation of a truncated Morse oscillator (Chem. Phys. Lett. **63**, 5 (1979)) used molecular parameters $\omega_e = 3104.3 \text{ cm}^{-1}$ and $X = 57.7 \text{ cm}^{-1}$, yielding $\omega_e = 3162.0 \text{ cm}^{-1}$, $C = 27.0$, and $D = 43319.4 \text{ cm}^{-1}$ ($D_0 = 41724.0 \text{ cm}^{-1}$). The results for the truncated 4 and 10 level systems in the H^{eff} model are, however, virtually identical with those shown in Ref. 10. It would appear that the anharmonicity X is the same but that there is a possible difference in the second Morse parameter D (or ω_e) used by us and that used by Schek *et al.* (Ref. 10). This has been confirmed by one of the authors of Ref. 10 [M. L. Sage (private communication)].
- ²⁰M. L. Sage (private communication).
- ²¹In Ref. 10, Δ was defined as $\Delta = (\omega_e - X) - \omega$, inconsistent with Refs. 18 and 19 which use $\Delta = \omega_{10} - \omega = (\omega_e - 2X) - \omega$ in accordance with Eq. (68). The H^{eff} resonance positions depend only on the anharmonicity X and not on the other Morse parameter D (or ω_e). Since our resonances for the four level system are coincident with those of Schek *et al.* (Ref. 10), we conclude that the spectra of $\log_{10} P_D$ vs Δ have been plotted in Ref. 10, according to Eq. (68). Further evidence for this is that the k -photon resonance position for a transition between molecular levels $i-k$ and i resulting from defining $\Delta = (\omega_e - X) - \omega$ is given by $\Delta = (2i - k)X$ which predicts that the ω_{10} one-photon resonance lies at $\Delta = X$ and gives *no* resonances at $\Delta = 0$. This is contradicted by the $\log_{10} P_D$ vs Δ spectrum for $N=4$ at lower intensity ($\omega_R = 1 \text{ cm}^{-1}$) in Fig. 2 of Ref. 10 [see also Fig. 1(a) of Ref. 20 to which this is practically identical]. The spectrum of average vibrational energy ($\log_{10} E_v$ vs Δ) is, however, plotted according to $\Delta = (\omega_e - X) - \omega$ in Ref. 10 [Fig. 4 of Ref. 10 is shifted by $+X \text{ cm}^{-1}$ from Fig. 1(b) of Ref. 19].
- ²²D. Proch and H. Schroder, Chem. Phys. Lett. **61**, 426 (1979).
- ²³P. Pechukas and J. C. Light, J. Chem. Phys. **44**, 3897 (1966).